Krzysztof Kotowski, Christoph Haskamp, Jacek Andrzejewski, Bogdan Ruszczak, Jakub Nalepa, Daniel Lakey, Peter Collins, Jose Martínez-Heras, and Gabriele De Canio

## **Technical Appendix**

1. Definitions	
1.1. Channel vs parameter	1
1.2. Subsystems	
1.3. Telecommands	
1.4. Target and non-target channels	2
1.5. Event class vs category vs type	
1.6. Event categories	
1.7. Event types	2
2. ESA Anomalies Dataset	3
2.1. Mission3	4
2.2. Examples of challenging events to detect	4
2.3. Annotation details	5
2.4. Anonymization details	6
2.5. Dataset structure	6
2.6. Comparison to related public datasets	7
3. Methods	9
3.1. Anomaly types	9
3.2. Metrics	
3.2.1. Analysis of metrics from the literature	11
3.2.2. Description of metrics priorities	
3.2.3. ESA-ADB metrics definitions	
3.2.4. Implementation details	
3.2.5. Approach for rare nominal events	15
3.3. Preprocessing	
3.4. Algorithms	
3.4.1. Telemanom adaptation (Telemanom-ESA)	
3.4.2. GlobalSTD	
3.4.3. DC-VAE and its adapted version (DC-VAE-ESA)	17
3.4.4. Experiments with transformers	
3.4.5. Algorithms' selection.	
3.4.6. Algorithms' parametrization	
4. Benchmarking results	
4.1. Example detections	
4.2. Results for anomalies only	
4.3. Results for lightweight test sets using algorithms trained on full sets	
4.4. Results for different mission phases	
4.5. Computational resources and limitations	
4.6. Processing times	
4. References	29

#### 1. DEFINITIONS

## 1.1. Channel vs parameter

Satellite telemetry consists of multiple time series that are called *parameters* by SOEs. This name is very problematic from the ML point of view because it collides with its fundamental nomenclature in which the *parameter* already has a couple of different meanings:

- a parameter of the model that is updated during the training, i.e., a single weight of the neural network;
- a parameter (or hyperparameter) of the algorithm which controls its behavior;
- a parameter of a statistical test (e.g., mean or variance of the estimated Gaussian distribution).

Hence, the *parameter* was replaced with the *channel* for purposes of ESA-ADB to avoid potential nomenclature collisions. *Channels* represent measurements from different sensors, status flags, and payload-related information. Each channel contains a list of samples defined by pairs of timestamps and signal values.

#### 1.2. Subsystems

Satellites are typically composed of multiple specialized parts (subsystems) including propulsion, electrical power, thermal control, attitude and orbit control, communication, and data handling subsystems. There are also unique satellite-specific subsystems in some missions. A subsystem gathers all components (and channels) responsible for a specific function.

#### 1.3. Telecommands

Telecommands (TCs) are sent from the Earth to the satellite in order to control different aspects of its operation. There are hundreds or thousands of different TCs for each mission with millions of total executions, affecting different subsystems and specific components. Many different TCs are frequently executed simultaneously or in series to perform specific instructions. They may affect the observed telemetry in various ways, from no visible changes to strong disruptions. In our dataset, each TC is a binary signal with values of 1 in the exact timestamps of TC's executions on-board the satellite. TCs are not expected to contain any anomalies and even if they were, anomalies (e.g., missing TCs) would be impossible to identify automatically without additional expert knowledge and information about mission plans. Thus, they are not monitored nor annotated for anomalies.

## 1.4. Target and non-target channels

Not every channel can be a target for anomaly detection benchmarking. Like telecommands, some channels are not expected to contain any anomalies, and it would be impossible to annotate them without additional external data anyway. Examples include status flags, counters, and metadata, such as location coordinates. They often contain important information in the context of anomaly detection but are not monitored nor annotated for anomalies. They may contain outliers that are, however, irrelevant (or nominal) for SOEs. They are called *non-target* channels in ESA-ADB. This aspect is usually not considered in existing multivariate anomaly detection datasets and benchmarks. The selection of *target* and *non-target* channels is somewhat subjective and it may turn out that some algorithms would be able to properly handle some *non-target* channels by discovering some unknown relationships in the data. However, the metrics in ESA-ADB are calculated only for *target* channels. *Non-target* channels may and should be used as input features for algorithms.

#### 1.5. Event class vs category vs type

Each annotated event can be assigned to a different class, category, and type:

- event classes relate to main causes of events and their specific variations (subclasses) as identified by SOEs. For example, attitude disturbances (with subclasses depending on the specific cause), resets, power drops, latch-ups, solar flares, etc.;
- *event categories* relate to the categorization of events from the operational point of view, i.e., anomalies, rare nominal events, communication gaps, and invalid segments, as described in the next section;
- event types relate to the signal characteristics of events according to the taxonomy introduced in Appendix Section 1.7.

Note that each feature is independent of others, that is, events of the same class can have different categories and types, e.g., resets caused by telecommands are categorized as rare nominal events, but unexpected non-commanded resets are categorized as anomalies.

#### 1.6. Event categories

For the purposes of our project, 4 categories of events are introduced: anomalies, rare nominal events, communication gaps, and invalid segments. They are defined in Table 5. The main reason was to distinguish atypical changes in the telemetry that should not be alarmed to operators (rare nominal events, communication gaps, and invalid segments) from unexpected ones that should be alarmed (anomalies). Rare nominal events are not anomalies from the operators' point of view and they are usually not reported in anomaly tracking systems. Eventually, they are recorded in the mission log as special operations. For some missions, i.e., Mission2, there is a significant number of such operations causing (not so) rare events. Hence, the ideal algorithm should not alarm for rare nominal events, but it is usually impossible to distinguish between novel rare nominal events and anomalies without additional a priori expert knowledge. As agreed with SOEs, it would be acceptable if an anomaly detection system shows a false alarm for the first occurrence of the specific rare event, but it should not alarm for any subsequent occurrences of similar rare events. In machine learning, we can define that problem as active one-shot learning. To enable evaluation in such a scenario using ESA-AD, it is necessary to distinguish rare events from anomalies in ground truth annotations. Besides, such a division allows us to calculate separate performance metrics for rare events and "real" anomalies. It also helps to interpret the results in case of false negative or false positive detections for rare events.

#### 1.7. Event types

To the best of our knowledge, the taxonomy by Blázquez-García et al. [1] is the only one in the literature that comprehensively defines multivariate anomaly types, and our definitions are built based on this foundation. It divides event types into point and subsequence ones, where point events are defined as single outlying data points. However, this definition does not take into

account varying sampling rates for which the length of "a single data point" may differ in time. Thus, for our purposes, multiinstance point anomalies are allowed if they are relatively short fragments of the signal that resemble points or peaks (i.e., up to 3
samples) when inspected using a typical sampling frequency for the channel. Both point and subsequence anomalies may be
univariate or multivariate depending on whether they affect one or more channels. Anomalies can additionally be divided into
global and local (contextual) ones, similarly as proposed in behavior-driven taxonomy by Lai et al. [2]. To make the original
definitions more specific in our taxonomy, the global subsequence anomaly is defined as a subsequence of anomalous values in
which at least one instance can be treated as a global point anomaly.

In the proposed taxonomy, each anomaly type can be described by three attributes: *dimensionality* (uni-/multi-variate), *locality* (local/global), and *length* (point/subsequence), as presented in Fig. 11. These attributes can be automatically inferred from perchannel annotations:

- 1. **Dimensionality** can be inferred by counting the number of channels affected by an anomaly. One affected channel makes it *univariate* and more affected channels make it *multivariate*.
- 2. To infer **locality**, we calculate the minimum and maximum values of all nominal samples in the dataset for each channel. If any sample of an annotated event lays out of <min, max> range for any channel, we mark it as *global*, otherwise it is *local*. This approach is a bit simplistic taking into account severe distribution shifts and different nominal levels of the signal in some missions, but it should be enough to identify *global* anomalies which could be detected with an out-of-distribution approach from more challenging *local* anomalies.
- 3. In terms of **length**, considering non-uniform sampling rates and the differences between mission and channels, it is hard to give a strict definition of a *point* anomaly. Our proposition is to make it dependent on the dominant sampling frequency for each mission (0.033 Hz for Mission1, 0.056 Hz for Mission2 and 0.065 Hz for Mission3). A point anomaly is defined as a sequence of up to 3 samples after signal resampling to the dominant sampling frequency. Importantly, some anomalies are fragmented into several non-overlapping annotated regions. In this case, we treat each region separately, so even if an anomaly contains several regions it can be a point anomaly if all of these regions are categorized as point anomalies.

Such automatically inferred attributes for every anomaly and rare event are given in anomaly\_types.csv for each mission, taking into account annotations for all channels. However, when working with subsets of channels, only the specific subset of channels should be considered to infer anomaly types. For this purpose, the script infer\_anomaly\_types.py is available in the code repository. The attributes are not inferred for communication gaps and invalid fragments.

TABLE 5
DEFINITIONS OF EVENT CATEGORIES

Event category	Definition	Typical examples	Alarming	
Anomaly	Atypical, rare, unplanned, and unwanted change in the telemetry.	Micrometeorite impacts, solar flares, hardware or software failures, latch- ups, unexpected responses to telecommands	Every occurrence should be alarmed.	
Rare nominal event	Atypical and rare but expected or planned change in the telemetry. It can be triggered by known telecommands (commanded rare event) or by any other non-commanded special event in the mission timeline.	Commanded: maneuvers, resets, calibrations, switching devices on/off  Non-commanded: planned autonomous operations, eclipses, lunar transitions	Only the first occurrence of a rare nominal event from each class may be alarmed. Subsequent occurrences should not be alarmed.	
Communication gap	Unusually long gap in the telemetry (missing data in some or all channels) not directly related to known anomalies.	Problems with the ground infrastructure, effects of resets	It should not be alarmed unless explicitly stated to do so.	
Invalid segment	Fragment of telemetry data containing invalid or forbidden values not directly related to known anomalies. It is neither nominal nor anomalous.	Telemetry does not meet clearly defined validity rules of the mission.	It should not be alarmed unless explicitly stated to do so.	

#### 2. ESA ANOMALIES DATASET

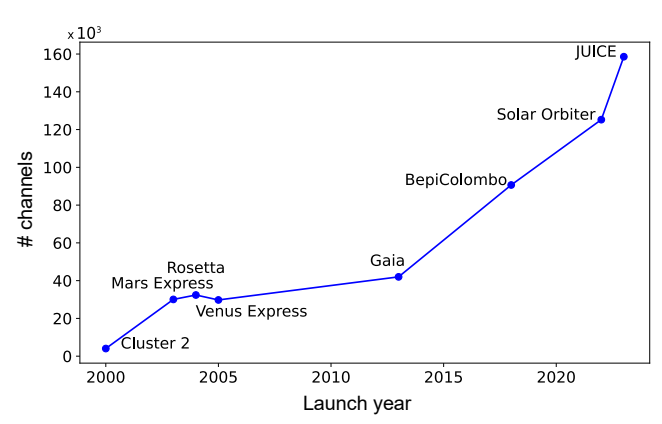


**Fig. 4**. Increasing complexity of selected ESA spacecrafts over time [3].

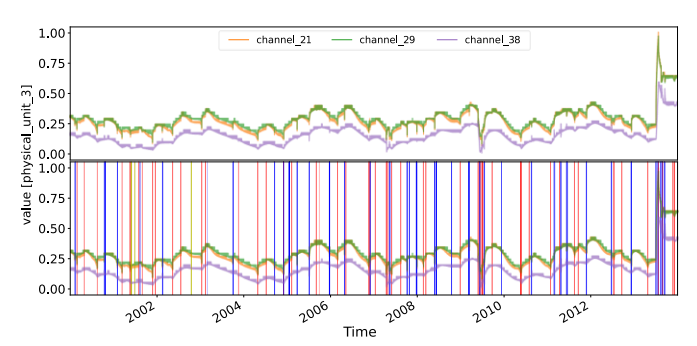


**Fig. 5.** Overview of 3 channels from group 4 in Mission1 without annotations (top panel) and annotated (bottom panel). Blue, yellow, and red vertical bars are rare nominal events, communication gaps, and anomalies, respectively.

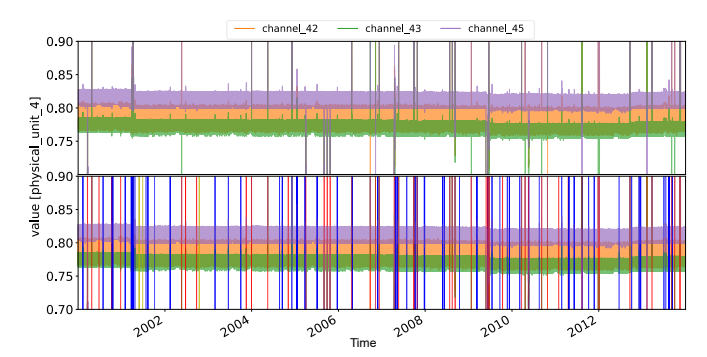


**Fig. 6.** Overview of 3 channels from group 8 in Mission1 without annotations (top panel) and annotated (bottom panel).. Blue, yellow, and red vertical bars are rare nominal events, communication gaps, and anomalies, respectively. The close-up of these channels is presented in Fig 2. in the main text.

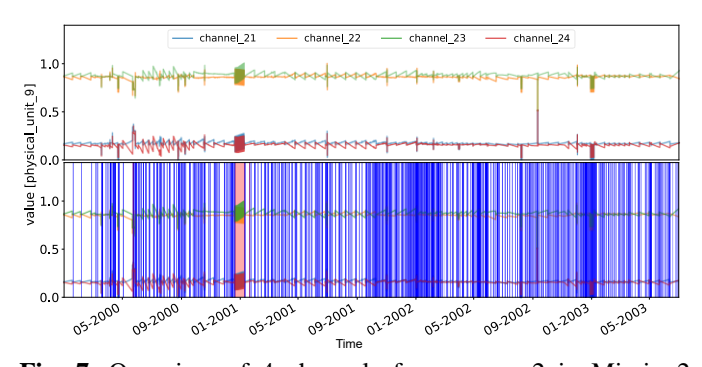


**Fig. 7.** Overview of 4 channels from group 2 in Mission2 without annotations (top panel) and annotated (bottom panel). Blue and red vertical bars are rare nominal events and anomalies, respectively.

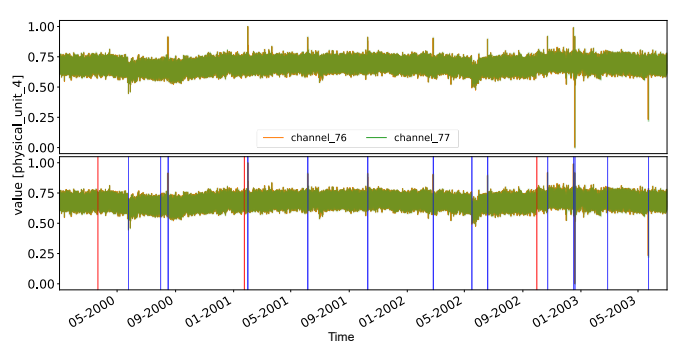


**Fig. 8.** Overview of 2 channels from group 31 in Mission2 without annotations (top panel) and annotated (bottom panel). Blue and red vertical bars are rare nominal events and anomalies, respectively. Note that channels have very similar values, so it is hard to distinguish them.

TABLE 6
MAIN CHALLENGES POSED FOR ALGORITHMS BY MISSIONS IN ESA-ADB

Mission	Main challenges for algorithms							
1	<ul> <li>Several anomalies are hard to spot (see Table 7)</li> <li>Several huge outliers (usually related to rare nominal events)</li> <li>Low signal-to-noise ratio in channels from group 8</li> <li>Monotonically non-decreasing signals in channels from group 2</li> <li>Last 18 months include a severe concept drift in channels from groups 4, 7, and 13</li> <li>There is a visible seasonality with a very long period length</li> <li>Overabundance of telecommands</li> </ul>							
2	<ul> <li>Several anomalies are hard to spot when looking at individual channels only (see Table 7)</li> <li>Overabundance of rare nominal events and a very small number of anomalies</li> <li>No obvious periodicity of the signal</li> <li>Monotonically non-decreasing signals in channels from group 20</li> <li>Many categorical and non-target channels</li> </ul>							

#### 2.1. Mission3

Mission3 is a part of ESA-AD but is omitted in ESA-ADB. It was omitted mainly because of many communication gaps (see Fig. 9), invalid segments (corrupted data), long periods of constant signals, lack of telecommands, and a small number of anomalies that are trivial to detect according to Definition 1 of Wu & Keogh [4]. However, it may still be an interesting resource for practitioners in the domain as it is fully annotated and contains a unique set of challenges related to satellite telemetry.

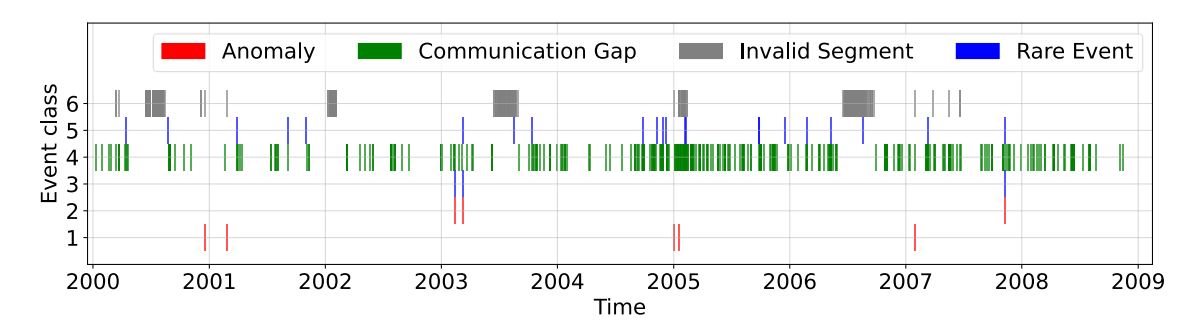


Fig. 9. Distributions of classes of annotated events across the timeline of Mission3.

## 2.2. Examples of challenging events to detect

As mentioned in the main text, the initial selection of missions was based on the presence of challenging anomalies according to SOEs. To support the analysis of results, a list of selected events of this type in test sets of ESA-ADB is provided in Table 7. It is not a complete list. It is limited to test sets and includes only subjectively selected examples among many others. Example detections by semi-supervised algorithms trained on full (suffix "-Full") and lightweight (suffix "-Light") subsets for selected events are presented in Appendix Section 4. as a series of figures referenced in Table 7.

Other interesting examples include events from classes 2, 14, 15, and 22 in Mission1 where similar changes in the same channel are sometimes categorized as anomalies and sometimes as rare nominal events, depending on the presence of TCs. A similar case for Mission2 is visualized in Fig. 10 for the non-commanded anomaly id\_618 and the commanded rare event id\_609. One of the important future works is to design algorithms that would be able to distinguish between such cases.

There are also some interesting nominal fragments related to atypical changes in sampling frequency in Mission1. There are 3 main examples of such behavior in the training set on days 2001-05-28, 2001-05-31, and 2001-06-27 where rapidly changing sampling rate causes small atypical "gaps" in data for channels 41-46. In the refinement process, it was observed that those gaps are detected as anomalies by many algorithms. However, we decided that they should not be annotated, because varying sampling rates are expected in satellite telemetry and these false detections are mainly since the selected algorithms are not aware of frequency changes.

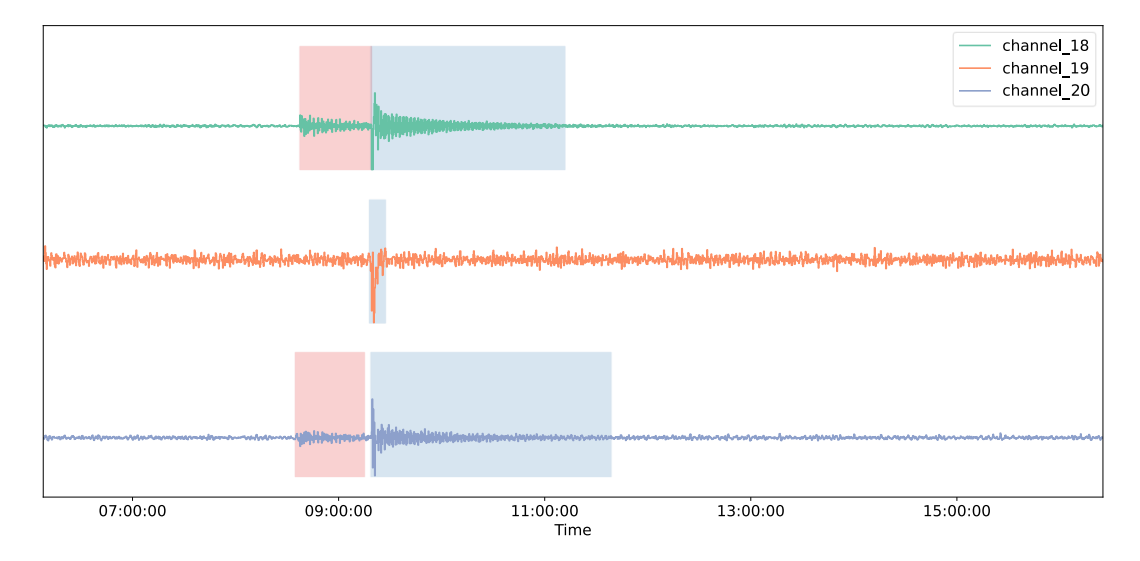


**Fig. 10**. Annotated anomaly id\_618 (marked in red) directly preceding the commanded rare nominal event id\_609 (marked in blue) in Mission2. The Y-axis is omitted, as channels are normalized and vertically shifted for improved visualization.

TABLE 7
LIST OF SELECTED CHALLENGING EVENTS ANNOTATED IN TEST SETS OF ESA-ADB

Mission	Event category	Event ID	Start time (YYYY-MM-DD hh:mm:ss)	Duration	Reason for selection
	Rare Event	id_24	2012-12-18 06:32:09	24h 15m	Hard to spot and not commanded. Not found by SOEs initially and added during the refinement process. It is related to a temporary change of nominal operational conditions.
	Rare Event	id_49	2011-10-08 07:08:39	10h 25m	Hard to spot, especially when looking at too narrow context. Caused by a rare TC. Fig. 17
	Rare Event	id_51	2011-08-14 19:12:39	1h 19m	Hard to spot, especially when looking at too narrow context. Caused by a rare TC. Fig. 18
	Rare Event	id_55	2011-04-23 08:19:39	0s (point)	Hard to spot in both lightweight and full sets. Caused by a unique execution of TC of priority 1. Overlaps with the rare event id_155.
Mission1	Anomaly	id_138	2009-10-13 06:39:17	1d 20h	Hard to spot using the lightweight subset of channels 41-46 only. Much easier to spot in channels 58-60. Fig. 19
Mis	Anomaly	id_153	2011-01-28 22:29:18	15h 14m	Hard to spot using the lightweight subset of channels 41-46 only. Much easier to spot in channels 64-66. Fig. 20
	Rare Event	id_155	2011-04-21 22:15:52	11d	Hard to spot using the lightweight subset of channels 41-46 only. Easier to spot in multiple other channels, but hard to accurately identify the start time due to very slow changes. Main text Fig 2. and Fig. 21
	Anomaly	id_157	2011-04-19 07:09:39	14h 35m	Hard to spot using the lightweight subset of channels 41-46 only. Much easier to spot in channels 64-66.
	Rare Event	id_159	2011-06-09 02:57:09	10d 21h	Hard to spot using the lightweight subset of channels 41-46 only. Very long annotations in other affected channels. Fig. 22
	Rare Event	id_466	2003-02-08 16:25:19	1h 10m	Small disturbance in 7 channels which may be easily overlooked, especially when using only the lightweight subset.
on2	Rare Event	id_591	2002-04-16 16:30:53	35m	Small disturbance in 7 channels which may be easily overlooked.
Mission2	Anomaly	id_631	2001-12-14 19:16:29	1h 18m	Small disturbance of unknown source in 7 channels which may be easily overlooked by operators. Fig. 23
	Anomaly	id_644	2002-02-18 05:42:45	9h 48m	Divergence of channel 81 from channel 73 which can only be detected when looking at both channels in the proper context window.

#### 2.3. Annotation details

While annotating, a special focus was put on the precise identification of anomaly starting points for all channels. On the other hand, anomaly end times may be less accurate, because they are much harder to identify objectively, especially for long anomalies. Importantly, ARTS reports are intended for human use and are not well-suited for ML purposes. They usually include only approximate time ranges and a small fraction of affected channels. Moreover, well-known anomalies and rare nominal events are often not reported. Thus, the whole signal was carefully revisited by the ML team in search of any suspicious events. An initial list of subsystems, channels, and telecommands relevant for anomaly detection was proposed by SOEs, but was gradually extended during several iterations of the annotation refinement process in which overlooked anomalies were discovered by the ML team using different TSAD algorithms. During this process, channels were divided into target and nontarget for anomaly detection. Non-target channels should only be used as additional information for the algorithms. They are not annotated and are not assessed in the benchmark. Examples include status flags, counters, and metadata such as location coordinates, where anomalies are not expected or it is not possible to check for anomalies without external data. Related channels measuring the same physical values and showing similar characteristics are organized into numbered groups, so it is easier to manage the dataset for ML purposes, e.g., to train group-specific models or to visualize results.

There are hundreds of different telecommands (TCs) in each mission. Some of them are critical for detecting annotated anomalies (i.e., when there is no reaction to the TC or the reaction is different than usual) or distinguishing anomalies from rare nominal events. However, it may be impractical to use them all in anomaly detection algorithms. Thus, 4 different priority levels for TCs were introduced as a suggestion about their potential usefulness for anomaly detection algorithms. The priorities from the least important to the most important are:

- 0. TCs not directly related to any subsystem included in the dataset.
- 1. TCs related to subsystems included in the dataset but not marked as potentially valuable for anomaly detection by SOEs.
- 2. TCs selected as potentially valuable for anomaly detection by SOEs.

3. A fraction of TCs of priority 2. assessed as valuable for anomaly detection by the ML team. The main rejection criteria were the scarcity of occurrences in the training data (less than 3) or no occurrences in the test data.

TCs of priority 3 are used as input for DC-VAE-ESA and Telemanom-ESA algorithms trained on full sets of channels. These priorities are only suggestions and ESA-ADB users are welcome to experiment with any combination of TCs.

## 2.4. Anonymization details

The anonymization had to be applied to conform with the ESA privacy policy and to avoid any accidental disclosure of sensitive mission-specific information or metadata. The anonymization process was carefully designed to maintain data integrity, so the results are independent of the anonymization. The following modifications were applied as a part of the anonymization process for each mission:

- Renaming of missions, subsystems, channels, telecommands, physical units, anomaly classes, and event types. They
  were consistently numbered according to their order of occurrence in files. Subsystems and physical units have
  consistent naming across missions, so it is possible to train cross-mission models.
- *Time scaling and shifting* of each mission. The timeline of every mission was scaled by a non-disclosed factor larger than 1 and shifted to start on 1<sup>st</sup> January 2000.
- *Normalizing values within channel groups to <0, 1> range.* Normalization per group was applied to preserve the same dependencies between similar channels before and after anonymization.

It was verified that the anonymization is fully reversible and there are no numerical errors related to the limited floating point resolution of values or timestamps. Additionally, it was verified that all deterministic algorithms in the benchmark produce the same results before anonymization.

#### 2.5. Dataset structure

ESA-AD consists of three folders, one per each mission. Each folder has the same structure presented in Table 8. There is a subfolder named channels and an optional subfolder named telecommands. Both subfolders include serialised and compressed Pickle files (docs.python.org/3/library/pickle.html, protocol version 4.0, zip compression), one for each channel and telecommand. Each file (pandas.pydata.org/pandascontains single pandas **DataFrame** docs/stable/reference/api/pandas.DataFrame.html, pandas version 1.5.3) including an index with consecutive timestamps and a single column with the corresponding raw telemetry values. Annotations of all events are in a separate file called *labels.csv* placed directly in the mission folder. It contains rows that describe anomalous fragments using 4 columns: the anomaly identifier (ID), the name of the channel affected by the anomaly, the start time, and the end time of the anomalous segment. Start and end times are defined as closed ranges and they usually represent timestamps of actual points in the dataset. There may be multiple segments with the same ID and channel name, but their time ranges cannot overlap. Additional information on anomalies can be found in the anomaly\_types.csv file. It describes each anomaly ID with its class, subclass, category, and type. The channels are described in the channels.csv file using the channel name, the associated subsystem, and the physical unit. The channel description also includes group numbers that indicate similar channels and the information if the channel is a target channel. If telecommands are included in the dataset their priority is described in the telecommands.csv file.

## TABLE 8 FOLDER STRUCTURE OF ESA-AD

- ESA-Mission/
  - channels/ folder including all channels of the mission
    - \*.zip compressed Pickle files for each channel
  - telecommands/ (optional) folder including all telecommands of the mission
    - \*.zip compressed Pickle files for each telecommand
  - labels.csv annotations
  - anomaly\_types.csv description of anomalies and rare nominal events
  - channels.csv description of channels
  - events.csv (optional) list of special operations and mission events
  - telecommands.csv (optional) description of telecommands

Some files are marked as optional, these files are not mandatory for the dataset or there might be missions not including these files. It should be possible to apply anomaly detection algorithms to the datasets not using the optional data, but it is expected that the optional data enhances the performance of algorithms when used. Mission2 includes an optional file *events.csv* which lists special operations and events with their start and end times according to the mission plan provided by SOEs. It was used to identify rare nominal events annotated in *labels.csv*, usually with slightly different start and end times due to different propagation times between channels.

## 2.6. Comparison to related public datasets

**Space-related dataset.** A quantitative comparison of the missions included in ESA-ADB and other public spacecraft-related telemetry datasets from the literature is presented in Table 9. There are 5 other public datasets of real-life spacecraft telemetry – 3 by NASA and 2 by ESA – and a single simulated one (CATS). The most popular ones are Soil Moisture Active Passive (SMAP) and Mars Science Laboratory (MSL) released by NASA [5]. According to the search for "SMAP" and "MSL" terms in Google Scholar since 2018, there are more than 200 documents that mention these datasets in the set of more than 500 citations of the source paper [5]. Besides a lot of criticism of these datasets in the recent literature [4], [6], [7], there is a common misconception about the number of channels included in these datasets. The data may come from 82 different physical channels in total, but there is a separate fragment for each channel without any synchronization with other channels, so they cannot be used effectively as a multivariate dataset. This is made clear in the description of the dataset in Table 9. NASA LASP WebTCAD [8] has tens of millions of points, but there are only 5 partially overlapping channels and no annotations of anomalies. ESA Mars Express Power Challenge [9] is popular in satellite telemetry forecasting, but does not contain anomalies annotations. The very recently published ESA OPSSAT-AD [16] is a toy dataset with 2213 univariate fragments of real OPS-SAT telemetry. It is contains anomaly annotations for whole fragments and is designed specifically for on-board applications.

Non-space-related datasets. There are also several related real-life datasets from outside the domain of satellite telemetry that are frequently used to benchmark multivariate TSAD algorithms. Notable examples include the Secure Water Treatment (SWaT) [10] and Water Distribution (WADI) [11] datasets which contain recordings from tens of channels from a real-world water treatment plant within several days. Server Machine Dataset (SMD) [12] including 5-week-long data from 38 parameters of 28 machines from 3 servers at a large internet company. The recent TELCO dataset [13] is worth noting due to related ideas of separate annotations for each channel, anomalies in training sets, and gradually increasing training set sizes. It contains 12 channels corresponding to real measurements collected over 7 months at an operation mobile internet service provider. To the best of our knowledge, the Exathlon benchmark [14], including real data traces from tens of repeated executions of streaming jobs with 2283 parameters (channels) on a Spark cluster over 2.5 months, is the only related dataset of volume comparable to ESA-AD, with more than 5 billion samples and 25 GB of data. However, it does not contain per-channel annotations and has been criticized for unrealistic anomaly density and positional bias [6].

Table 10 gives qualitative description of how ESA-ADB addresses main 4 flaws reported by Wu & Keogh [4].

TABLE 9
QUANTITATIVE COMPARISON OF ESA-AD AND OTHER PUBLIC SPACECRAFT DATASETS.

Dataset name	Number of channels	Total volume	Number of annotated events
ESA-AD (Ours)	Mission1: 1 fragment with 76 channels and 698 commands  Mission2: 1 fragment with 100 channels and 123 commands	1,551,591,259 samples 3,512,724 commands executions	842 (1.17% of all samples)
NASA SMAP and MSL [5]	SMAP: 55 fragments with 1 channel and 24 commands  MSL: 27 fragments with 1 channel and 55 commands	706,971 samples 410,030 commands executions	105 (8.98% of all samples)
NASA LASP WebTCAD [8]	1 fragment with 5 partially overlapping channels	55,258,122 samples	not annotated
NASA Shuttle Valve Data (cs.fit.edu/~pkc/nasa/data)	<b>TEK</b> : 12 fragments with 1 channel <b>VT1</b> : 27 fragments with 1 channel	552'000 samples	8 whole fragments
CATS [15] (simulated)	1 fragment with 17 channels	85,000,000 samples	200 (2.15% of all samples)
ESA Mars Express Power Challenge [9]	Train: 3 fragments with 38 channels (including 5 metadatarelated)  Test: 1 testing fragment with 5 metadata channels	198,045,083 samples	not annotated for anomalies
ESA OPSSAT-AD [16]	2123 univariate fragments from 9 different channels	303,493 samples	434 whole segments (20.44%)

TABLE 10 A LIST OF FLAWS REPORTED BY Wu & 2.6 [4] AND HOW THEY ARE ADDRESSED BY ESA-ADB.

A LIST OF FLAWS REPORTED BY WU & 2.0 [4] AND HOW THEY ARE ADDRESSED BY ESA-ADD.					
Flaw	How does ESA-ADB address it?				
Triviality	<ul> <li>ESA-AD is large and contains a diverse set of anomaly types and concept drifts which hamper the usage of simple algorithms</li> <li>ESA-AD offers a selection of non-trivial anomalies, so they can be evaluated separately (Appendix Section 2.2)</li> <li>ESA-ADB includes a set of simple algorithms to verify the potential triviality of anomalies</li> </ul>				
Unrealistic anomaly density	<ul> <li>ESA-AD is large and the anomaly density in the dataset is below 2% of data points</li> <li>There are only dozens of anomalous events per year</li> <li>Series of separate annotated segments within a short region are usually assigned to the same event and are treated as such when computing metrics</li> </ul>				
Mislabelled ground truth	While this flaw cannot be fully resolved in real-life datasets there were several iterations of the annotation refinement process aided by unsupervised and semi-supervised algorithms to identify potential mislabelling [17]				
Run-to-failure bias	<ul> <li>Anomalies are scattered across long, failure-free, operational periods of acquired telemetry data from real satellite missions</li> </ul>				

#### 3. Methods

#### 3.1. Anomaly types

Fig. 11 gives an overview of the proposed taxonomy of anomaly types and Table 11 gives statistics of each anomaly types across all missions in ESA-AD.

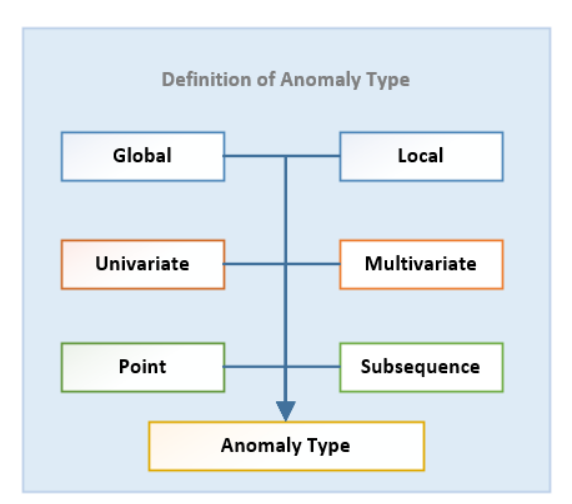


Fig. 11. Anomaly types considered in ESA-ADB.

 $\label{eq:table 11} TABLE~11$  Distribution of 8 combinations of anomaly types across missions

Length	Locality	Dimensionality	Mission1	Mission2	Mission3
	Global	Univariate	0.00%	0.00%	9.09%
Point	Giobai	Multivariate	5.10%	0.00%	0.00%
Point	Local	Univariate	0.51%	0.00%	0.00%
		Multivariate	0.51%	0.00%	0.00%
	Global	Univariate	12.24%	0.00%	60.61%
Subsequence	Global	Multivariate	40.31%	90.84%	15.15%
	Local	Univariate	3.57%	1.40%	6.06%
	Local	Multivariate	37.76%	7.76%	9.09%

## 3.2. Metrics

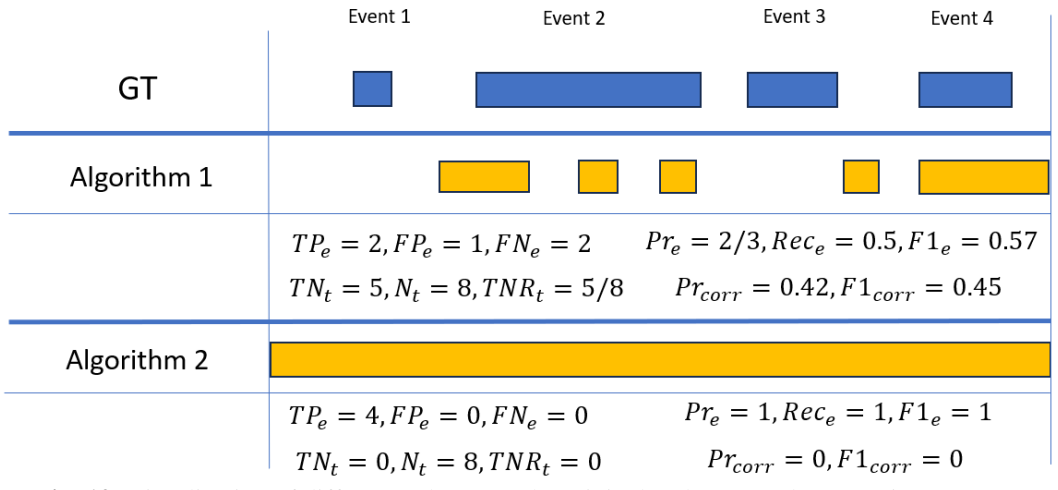


Fig. 12. Visualization of differences between the original and corrected event-wise F-scores.

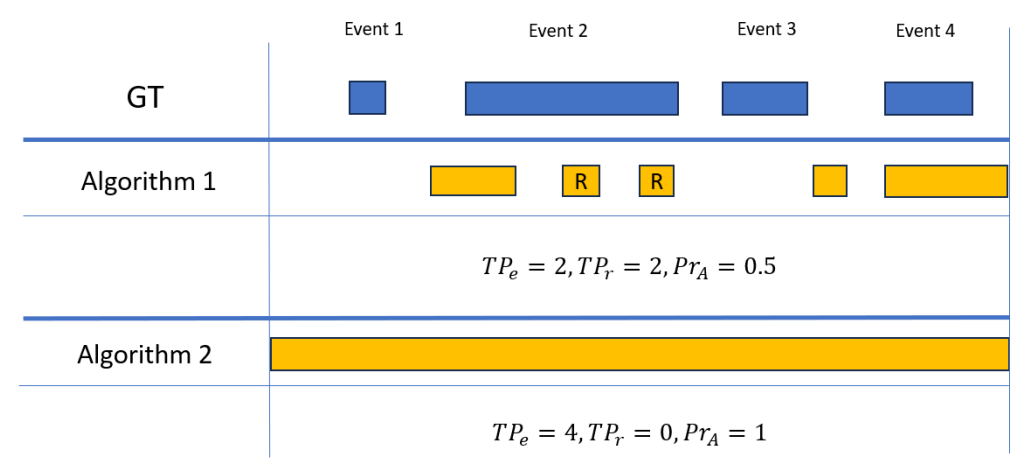
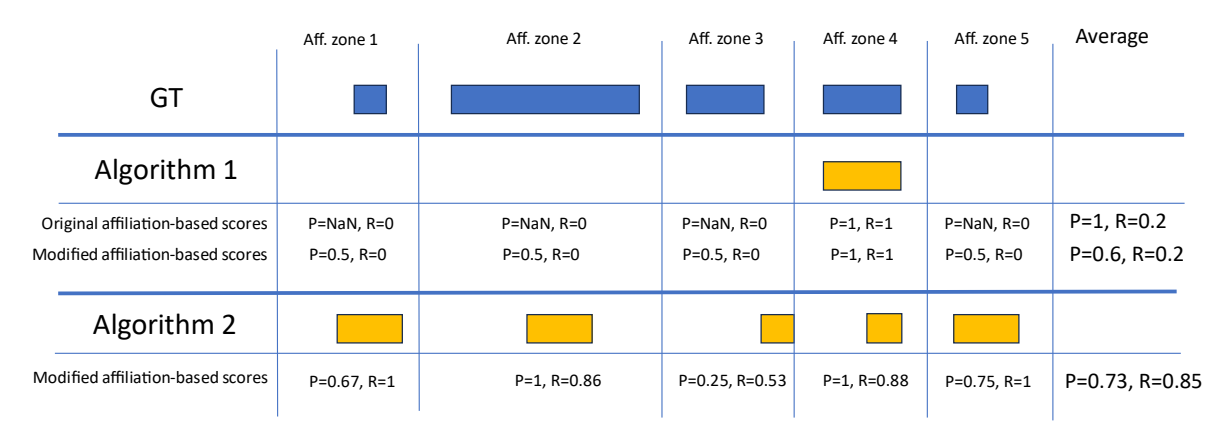


Fig. 13. Visualization of the event-wise alarming precision calculation.



**Fig. 14.** Visualization of differences between the original and modified affiliation-based scores on a simulated example. (P – precision, R – Recall)

## 3.2.1. Analysis of metrics from the literature

There are some recent comprehensive reviews of TSAD metrics in the literature [18], [19]. It is an active area of research in which many new approaches were introduced recently. However, none of these metrics is universal, they focus on different aspects of detection quality which may differ between applications. Table 12 gives an overview of our analysis of state-of-the-art metrics together with their pros and cons in the context of satellite telemetry anomaly detection.

TABLE 12

Analysis of existing metrics from the literature with reasons for inclusion/exclusion in ESA-ADB

ANALYSIS OF EXISTING METRICS FROM THE LITERATURE WITH REASONS FOR INCLUSION/EXCLUSION IN ESA-AD						
Category	Metric	Included in ESA-ADB	Reason for inclusion/exclusion			
Sample-wise	All classic precision-based and recall-based metrics treating each time point as an independent sample	No	Simple per-sample metrics are not aware of temporal aspects of time series in which anomalies are usually continuous sequences of correlated samples (like a vast majority of anomalies in satellite telemetry). This leads to multiple problems with a proper assessment of algorithms, i.e., longer anomalies are getting more importance than shorter ones, and close detections are not rewarded.			
	NAB score [20]	No	It is only applicable to domains where an anomaly is a single sample rather than a series of samples. Moreover, there are certain ambiguities in the scoring functions and magic numbers for its parameters [21].			
	Point-adjust [22]	No	It is recently widely criticized for various reasons [23], [23], [24], [25], [26]. Mainly because it is overly optimistic and even a random anomaly score can reach state-of-the-art results in this metric in specific adversarial cases [23], [24], [26]. Also, it gives more importance to longer anomalies and is unable to give a larger score to a model which finds the true range of the anomaly better.			
	Event-wise score [5]	No	It is improvement of point-adjust approach which partially solve the problem with higher importance of long anomalies, i.e., long anomalies have the same "weight" as short ones, but there is still a much higher probability that a random detector will detect the longer anomaly. Moreover, an algorithm that simply detects anomalies for every sample in the dataset would have a perfect event-wise precision.			
Range-based	Composite F-score [27]	No	It calculates the precision in a per-sample manner and recall in an event-wise manner, so it still gives smaller weights to short false positives which are equally or more annoying than longer ones.			
, ä	Corrected event-wise F-score [26]	Yes	It resolves issues with the event-wise precision using a correction for per-sample true negative rate. It increases importance of short false positives and penalizes overly long detections.			
	Precision and Recall for Time Series [28]	No	It requires 4 hyperparameters to be tuned. The recall is not monotonically decreasing with an increasing threshold. Such a behavior can even lead to problems when computing aggregated metrics that assume recall consistency [6]. Its calculation time does not scale well for large datasets.			
	TaPR and eTaPR [23]	No	It requires 3 hyperparameters and its calculation time does not scale well for large datasets.			
	Affiliation-based score [24]		It is parameter-free, locally and statistically interpretable, robust to "adversary" predictions, and scales well for large datasets.			
	Volume Under the Surface [29]	No	It operates on continuous anomaly scores and we require binary outputs. It has very high computational complexity and does not scale well for large datasets.			
ı timing	Early Detection [30]	No	It assumes that anomalies can only be detected within the ground truth interval – <i>after</i> they appear in the signal. It does not account for too early detections which may be treated as false positives by spacecraft operators.			
Detection timing	Before/After-TP [31]	No	This approach requires calculation of two different values (Before-TP and After-TP) which are not obvious to aggregate to assess the overall detection timing quality. Moreover, it is impossible to calculate both values for every detections.			

nomaly diagnosis (Channels identification)	HitRate@P% [12]	No	It needs information about the relative relevance of detections that is not available when using binary outputs. It does not penalize models detecting too many channels. To always achieve a score of 1 model can simply mark all channels as anomalous. It is a crucial problem in satellite telemetry because we aim to mark only relevant channels to investigate by space operations. Any additional irrelevant detections should be penalized.
Anomaly dia	Normalized Discounted Cumulative Gain [32]	No	It needs information about the relative relevance of detections that is not available when using binary outputs.

#### 3.2.2. Description of metrics priorities

The highest priority aspect relates to the proper identification of anomalous events, but with a strong emphasis on avoiding false alarms at the same time (aspects 1a. "No false alarms" and 1b. "Anomaly existence" in Table 3 in the main text). This is because false positives are costly to resolve and deter operators from using the system. A high false positive rate is reported in the literature as the main obstacle to the wider adoption of anomaly detection algorithms in space operations [5]. This fact additionally supports our idea of hierarchical evaluation, since a high false positive rate disqualifies an algorithm even if it obtains perfect scores in other aspects. Moreover, most other aspects focus only on performance for true positive detections (i.e., channel identification, alarming precision, timing quality), so they indirectly depend on the anomaly existence aspect.

The second highest priority for SOEs is to have information about subsystems and channels affected by anomalies (aspects 2a and 2b). Proper subsystem identification is more important for SOEs as it gives a more concise overview of the situation than a long list of specific affected channels. Again, it is of paramount important to avoid false positives. It is strongly preferable to miss some channels rather than to wrongly identify many irrelevant channels. ESA-AD contains tens of target channels which is already hardly manageable for manual analysis, moreover, it is just a fraction of channels from actual missions. Hence, an algorithm which does not provide affected channels is of low practical utility, or even worse, it may amplify the "black box" nature of advanced algorithms and decrease trust in this kind of system among operators. That is why it was considered as the second of two *primary* aspects of highest priority.

The following 3 *secondary* aspects are not so crucial for SOEs but are certainly useful to differentiate between algorithms having the same *primary* scores. The 3<sup>rd</sup> priority is to avoid algorithms that frequently repeat alarms for the same continuous anomaly segment (aspect 3. "Exactly one detection per anomaly"). It is strongly connected to the 1a. "No false alarms" priority, because even if all repeated alarms are true positives, they would be annoying and confusing to operators, nearly as badly as false positives. The last 2 priority levels directly relate to the anomaly detection timing. It is better to detect anomalies earlier than later (aspect 4. "Detection timing"), it is preferable to detect a whole time range of an anomaly instead of just a part of it, and, in case of false detections, it is better to show them close to real anomalies (aspect 5. "Anomaly range and proximity"). These aspects are often highly emphasized in TSAD benchmarks from the literature, e.g., NAB [20] and Exathlon [14]. However, they are relatively less important for on-ground mission control. Additionally, the latter aspect cannot be precisely assessed due to the problems with the objective identification of anomaly end times (discussed in Appendix Section 2.3).

## 3.2.3. ESA-ADB metrics definitions

The definitions of the proposed metrics are given in the following paragraphs. All implementations are available in the published code. All metrics are defined in the <0, 1> range where 1 is the perfect score. Technical details of implementations are listed in Section 3.2.4.

**Subsystem/channel-aware F-scores.** Typical TSAD metrics are applicable only in univariate settings. To get a single score for multiple channels, there must be some aggregation performed. Such aggregation loses information about the performance for individual subsystems or channels, so it is impossible to assess their correct identification. In recent articles [33], [34], special anomaly diagnosis metrics are proposed to address this issue, namely *HitRate* and *Normalized Discounted Cumulative Gain*. These metrics measure how relevant are the detected channels according to the list of annotated channels. However, they need information about the relative relevance of detections which is not available when using binary outputs. Thus, a new approach is proposed based on precisions and recalls of identifying the list of affected subsystems and channels.

SOEs inspect potential anomaly sources at two levels of detail. First, they check which subsystems are affected by the anomaly. Later on, they look at the specific channels affected in those subsystems. The usefulness of algorithms supporting such inspection is proposed to be measured with *subsystem-aware* (SA) and *channels-aware* (CA) F-scores. A subsystem is counted as true positive  $(TP_{SA})$  if it has at least one annotated channel and at least one detected channel (not necessarily the same) overlapping with the full time span of an event. A subsystem is considered a false negative  $(FN_{SA})$  if it has at least one annotated channel but no such detections. A false positive subsystem  $(FP_{SA})$  has no annotated channels but has at least one such detection. Thus, the *subsystem-aware* F-score  $F_{\beta_{SA}}$  is given by (3).

$$F_{\beta_{SA}} = (1 + \beta^2) \frac{Pr_{SA} \cdot Rec_{SA}}{(\beta^2 \cdot Pr_{SA}) + Rec_{SA}},$$

$$Pr_{SA} = \frac{TP_{SA}}{TP_{SA} + FP_{SA}}, \quad Rec_{SA} = \frac{TP_{SA}}{TP_{SA} + FN_{SA}}$$
(3)

The *channel-aware F-score* is defined analogously, taking into account separate channels instead of subsystems. Again, 0.5 is used for  $\beta$  as a baseline to be consistent with the event-wise F-score. For the lightweight subsets of channels (selected from a single subsystem), the subsystem-aware F-score is not reported.

**Event-wise alarming precision.** The corrected event-wise F-score counts only a single true positive even if there are multiple separated detections for the same fragment in the ground truth (Fig. 13). In practice, such redundant detections may cause repeated alarms which may be annoying for operators. The *event-wise alarming precision* measures the ratio of correctly detected events to the sum of correctly detected events and redundant alarms. This metric may seem too strict in some cases, i.e., many short detections close to each other, but it represents a practical aspect of mission operations and encourages applying better thresholding or postprocessing approaches to avoid redundant alarms.

Anomaly detection timing quality curve (ADTQC). The goal of this novel metric is to assess the accuracy of the anomaly start time identification from the SOEs point of view. Some existing metrics of the anomaly detection latency, such as *After-TP* [31] or *Early Detection* (ED) [30], assume that an anomaly can be detected only within its ground truth interval – *after* it appears in the signal. However, the question arises how to assess algorithms that detect anomalies too early – *before* they start. They cannot be assessed using *After-TP* or *ED* metrics but they certainly have some value. The *Before-TP* metric [31] and the *NAB score* [20] rank earlier anomaly *predictions* (to distinguish them from *detections*) as better. However, in practice, as suggested by SOEs, too-early detections may be seen as false positives by operators if they cannot confirm the existence of an anomaly within a definable time. Thus, too early detections may decrease operators' trust in an algorithm and, in this context, are much worse than late detections of comparable distance from an anomaly start time. According to SOEs, the quality of anomaly detection timing should decrease exponentially for detections before the actual start time as opposed to much slower degradation of quality for moderately late detections. A survey was conducted and confronted across SOEs from different missions in ESA and KP Labs to define the timing quality in the range from 0 to 1 as a function of detection start time. The resulting consensus reflecting the common operators' point of view is reflected in the ADTQC described by Appendix Equation (4) in Appendix Section 3.2.2.

Modified affiliation-based F-score. The affiliation-based approach by Huet et al. [24] claims to resolve all the major flaws of previous range-based metrics. That is, it is aware of the temporal adjacency of samples and anomalies duration, has no parameters, and is locally and statistically interpretable. The main idea is to divide ground truth into local zones affiliated with consecutive anomaly ranges. The borders of such affiliation zones lie in midpoints between consecutive anomalies. Precision and recall are calculated separately for each affiliation zone based on the average directed distance between sets of annotated and detected points, either the distance from annotated to detected (precision) or from detected to annotated (recall). Affiliation-based F-score with  $\beta$  of 0.5 is calculated to underscore the strong practical need to minimize the number of false positives. The final global F-score is calculated as the arithmetic average of all local F-scores (with each affiliation zone having the same weight). The important modification to the original implementation relates to frequent situations when it is impossible to calculate the precision in an affiliation zone (when there is no detection there are no true positives or false positives). In the original formulation, such an affiliation zone was simply ignored when calculating an average precision over all affiliation zones. However, this approach makes it hard to robustly compare different algorithms because of the different numbers of affiliation zones taken into account, e.g., it gives a higher score to an algorithm that detects a single anomaly very precisely and misses 4 others than to an algorithm that detects all 5 anomalies relatively well – see Fig. 14. In our formulation, empty detections get a precision of 0.5. Such a value can be interpreted as a random detection, so this modification promotes algorithms that would rather give an empty detection than a false detection that is worse than random. There are also some other technical adaptations to handle point anomalies and fragmented annotations, as described in Appendix Section 3.2.2.

#### 3.2.4. Implementation details

**Operating in the time domain**. ESA-AD has varying sampling rates and we keep them on purpose to maintain the true characteristics of satellite telemetry data. Our evaluation pipeline should handle this issue to consistently evaluate the results of algorithms using different sets of timestamps on the output. The only way to achieve this is to use metrics operating in the time domain instead of the samples domain, so that the ground truth and the detections can use completely different sets of timestamps (of different lengths and varying sampling rates). Original implementations of most metrics do not support timestamped arrays. They assume that the ground truth and the detections have the same uniformly sampled timeline. Our metrics operate on arbitrarily timestamped ground truth and detection arrays (possibly of different lengths and sampling frequencies). Hence, no matter the sampling frequency used in the algorithm, the metrics are always calculated relative to the original non-uniformly sampled ground truth. For operations on time ranges, we use the *portion* library (github.com/AlexandreDecan/portion).

**Timestamps as real numbers.** Our modified version of the affiliation-based metric operates on timestamped arrays, but the timestamps are transformed into the number of nanoseconds since the beginning of the dataset, so the internal implementation of the affiliation-based score is unchanged (it can operate on real numbers only). Additionally, point events (with the same start and

end times) are adjusted, so that the end time is 1 nanosecond later than the start time. Such modification had to be applied because the affiliation-based score cannot be calculated for point events of zero length. The same point anomalies adjustment was applied to the channel-aware F-scores.

Multiple annotations for the same event. It is a common situation in our dataset that multiple non-overlapping fragments close to each other are annotated with the same event ID (e.g., Fig 2. in the main text). This is usually because the source of the anomaly is the same for all fragments. In such cases, we should treat all fragments as a single anomaly (i.e., when selecting affiliation zones and calculating distances) as suggested in recent literature [4], [24]. To implement such correction in the affiliation-based score without changing its internal assumptions and implementation, a macro-averaging across anomaly IDs was introduced, i.e., it first aggregates zones affiliated with the same anomaly IDs by averaging their precision and recall scores and then calculates an average across all anomaly IDs. It also affects the implementation of the alarming precision metric which does not penalize redundant detections belonging to non-overlapping ground truth fragments.

Overlapping events. There are several cases in our dataset where annotations of different events for the same channel are overlapping in time, i.e., when an anomaly occurred during a longer rare event. The affiliation-based metric is unable to separate such events because it is impossible to create non-overlapping affiliation zones for them, so there are no corrections for this situation to not interfere with the main principles and assumptions of the metric. For subsystem-aware and channel-aware metrics, each event is analyzed separately, i.e., separate true positives and false negatives are counted for each event. Moreover, any false positives related to correct detections of other overlapping anomalies are discarded.

ADTQC details. The anomaly detection timing quality curve (ADTQC) is defined by (4) and visualized in Fig. 15.

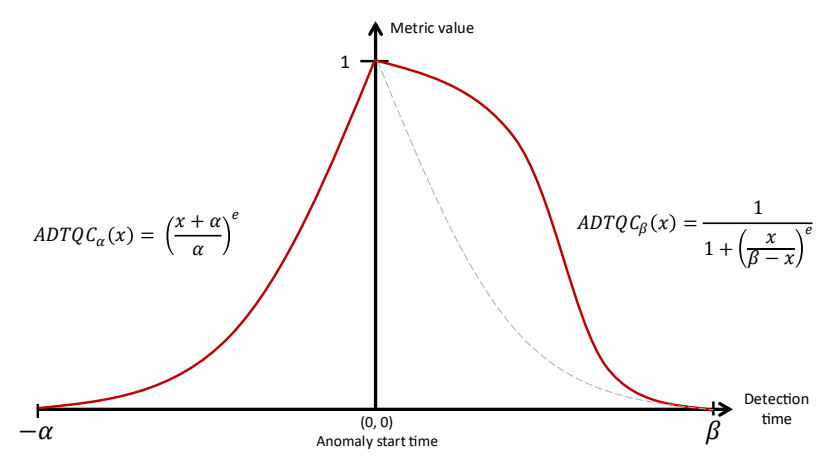


**Fig. 15.** Anomaly detection timing quality curve (ADTQC).

$$ADTQC(x) = \begin{cases} 0, & -\infty < x \le -\alpha \\ \left(\frac{x+\alpha}{\alpha}\right)^e, & -\alpha < x \le 0 \\ \frac{1}{1+\left(\frac{x}{\beta-x}\right)^e}, & 0 < x < \beta, & \alpha, \beta > 0 \end{cases}$$

$$ADTQC(x) = \begin{cases} 0, & x \ne 0 \\ 1, & x = 0 \end{cases} \quad (\alpha = 0 \land x \le 0) \lor (\beta = 0 \land x \ge 0)$$

$$(4)$$

 $\alpha = \min(anomaly\ length, anomaly\ start\ time - previous\ anomaly\ start\ time)$ 

 $\beta$  = anomaly length

After agreeing on the shape of ADTQC, the most important issue was to select the operational range of values for which the function should return a quality higher than 0, that is, for which the detection is not useless from the practical point of view. The first straightforward step was to define detections later than the anomaly end time  $(\beta)$  as useless. Accordingly, detections earlier than the anomaly length from the start time were also considered useless. Hence, the shorter the anomaly the more accurately it must be detected to achieve similar quality value. In the extreme case of point anomalies, ADTQC returns a value of 1 for exact detections and 0 otherwise. It makes sense from the practical point of view for two reasons, 1) detections for short, hardly noticeable anomalies are likely to be considered false alarms if not well-timed, and 2) end times of long anomalies are usually much harder to annotate precisely than for short anomalies. Another unacceptable situation was identified when a detection is earlier than the previous anomaly start time. When anomalies are close to each other, the detection timing must be even more accurate to ensure their better separation.

The ADTQC metric value for the specific anomaly is determined by simply calculating the value of the ADTQC(x) function where x is the difference between the detection start time and the anomaly start time. Similarly to Before/After-TP [31], the metric is calculated and averaged across all correctly detected events to get a final score in the range from 0 to 1. To support the analysis of the results, the ratio of detections after the anomaly starting points to all detections is calculated (called the *after ratio*).

For multivariate anomalies, the ADTQC metric is calculated between the logical sums of annotations and detections across all target channels. It does not matter if the detections are for correct channels because the metric focuses on the timing alone. The second possible approach in the multivariate setting would be to calculate the ADTQC metric for each affected channel separately. The average across all affected channels would be the final ADTQC score for a specific anomaly. While this alternative approach would allow for more detailed quantification of the anomaly detection timing across channels, it does not reflect the operators' perspective in which the first detection is the most important one, because it already enforces an action. Later detections for any other channel do not matter so much, because operators are already aware of the potential anomaly.

All metrics can be calculated excluding some specific event categories, classes, or types. For the corrected event-wise F-score, detections for excluded events are ignored when counting true and false positives, and a lack of detection is not counted as a false negative for them. For other metrics, excluded events are simply not considered when calculating the mean across events.

#### 3.2.5. Approach for rare nominal events

Most algorithms in the TimeEval framework (and in the literature) do not support learning rare nominal events explicitly (i.e., by one-shot learning or keeping rare events in memory). For such standard algorithms, rare events will always be detected as anomalies, so for simplicity, rare nominal events are treated as anomalies in the current benchmark. However, we strongly encourage to use ESA-AD to design models that learn nominal rare events and avoid detecting them in the future, which would be of high practical importance for mission control. For this purpose, we propose a framework to assess them:

- 1) The first detection of a novel rare nominal event (not seen during training) should not be penalized. However, the algorithm should be able to actively learn from the operators' feedback (i.e., "this is not an anomaly") and should not detect similar events in the future (one-shot learning).
- 2) For known rare events (seen during training or actively learned during inference), every subsequent detection should be penalized, i.e., we should minimize per-event false positive rate (FP / (FP + TN)) where FP is falsely detected rare event and TN is a correctly undetected rare event.

## 3.3. Preprocessing

Fig. 16 presents an example of the proposed zero-order hold resampling scheme. It is implemented as follows:

- 1. Construct a uniformly sampled list of timestamps in the target sampling frequency. Set the first/last timestamp in the list to the value of the earliest/latest original timestamp across all channels rounded down/up to the target sampling resolution. Fill the list between the first and the last element using uniformly sampled timestamps in the target frequency, e.g., if we resample a list of original timestamps <8:10:12, 8:10:14, 8:10:38> to the target frequency of 1/10 Hz (target resolution of 10 seconds), the resampled list will be <8:10:10, 8:10:20, 8:10:30, 8:10:40>.
- 2. Propagate the last known value and label from the original samples (zero-order hold) to each timestamp in the constructed list. If there are still any missing values for the initial element of the list (i.e., when some channels start a little earlier than others), backpropagate the first known value from the original samples. This introduces a bit of information from the future, but it usually concerns only a few samples at the beginning of a test set.
- 3. Apply a correction for missing anomalies to ensure that no point events are removed due to the resampling. Iterate through consecutive pairs of unannotated timestamps in the resampled list and, if there are any annotated original points in between, take the last annotated sample and assign its value and label to the latter timestamp from the pair. The result of such a correction is visible in the rightmost sample of Channel 1 in Fig. 16.

Target sampling frequencies have been selected separately for each mission (0.033 Hz, 0.056 Hz, 0.065 Hz, for Missions 1, 2, 3, respectively) based on the analysis of the most densely sampled target channels to prevent losing any annotated anomalies, especially point anomalies.

Channels with categorical values and status flags are enumerated according to the order of occurrence of each state in the training set before standardization. This is a very naïve approach, but it does not require laborious manual analysis of all channels and preparation of state mappings for each potential mission. Also, it does not require special handling of categorical anomalies. Moreover, categorical channels are usually non-target.

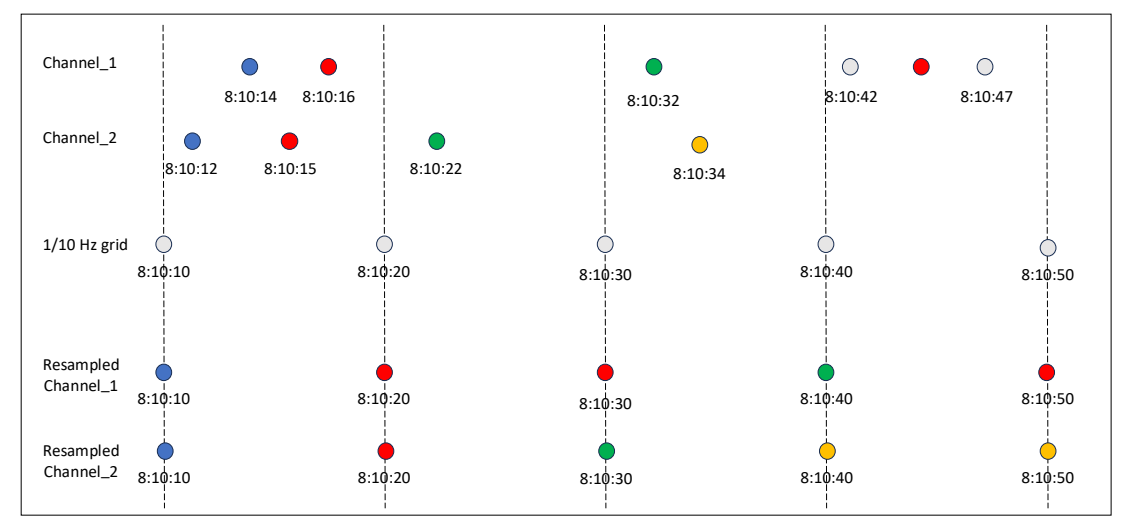


Fig. 16. Visualization of our resampling procedure for two non-uniformly sampled channels. Colors represent different values of the signal for each channel.

#### 3.4. Algorithms

This section provides all details on algorithms implementation, selection, and parametrization in the benchmark.

## 3.4.1. Telemanom adaptation (Telemanom-ESA)

The semi-supervised Telemanom algorithm proposed by NASA engineers [5] is an important point of reference in the domain. It can be considered the most popular algorithm for anomaly detection in satellite telemetry. Its core element is an LSTM-based RNN that learns to forecast a small number of time points (10 by default) for a single channel based on the hundreds of preceding samples (250 by default) from multiple input channels. The mean absolute difference between the forecasted samples and the real signal is treated as an anomaly score, which is thresholded using the non-parametric dynamic algorithm (NDT) to find anomalies. However, this "non-parametric" approach (in the sense that it does not use Gaussian distribution parameters to estimate thresholds) has several hyperparameters. In one of our previous works, a genetic algorithm was used to find optimal hyperparameters [35]. However, this wrapper approach would be too computationally expensive to run on our large datasets, so the default settings proposed by the authors were used.

Our proposed *Telemanom-ESA* solves several technical issues of the original Telemanom identified when working on ESA-ADB, including memory inefficiency, magic numbers causing problems in thresholding (*Telemanom-ESA-Pruned*), no proper handling of anomalies in training data, and a lack of scalability to hundreds of channels.

- Memory inefficiency Telemanom was designed for small and simplified datasets provided by NASA. Hence, the code is not optimized to handle very large datasets and it results in out-of-memory errors, e.g., there are many unnecessary copies of data, all training windows are loaded into memory at once, and binary annotations are loaded to memory as floating-point numbers. **Telemanom-ESA:** The code is optimized for memory consumption by using lazy generators to prepare training batches, in-place operations instead of copying data to new variables, and optimized data types.
- Magic numbers in thresholding there are several conditions in the thresholding code that are not well documented in the original article. Especially impactful is that windows with smoothed errors below 0.05 are never anomalous (<a href="mailto:github.com/khundman/telemanom/blob/26831a05d47857e194a7725fd982d5dea5402dd4/telemanom/errors.py#L339">github.com/khundman/telemanom/blob/26831a05d47857e194a7725fd982d5dea5402dd4/telemanom/errors.py#L339</a>). This is a very data-specific condition that is not well-suited for channels with certain signal values. **Telemanom-ESA:** This specific condition was removed from the code. **Telemanom-ESA-Pruned:** The threshold of 0.05 is much too high for ESA-ADB, so it was changed to 0.007 based on the manual analysis of smoothed errors in the training data of both missions. This selection is highly subjective and is probably not optimal, but allows to assess the effect of such a pruning on the results.
- No proper handling of anomalies in training data Telemanom assumes that there are no anomalies in the training set which is not true in our real-life setting. **Telemanom-ESA**: only continuous nominal parts longer than 260 samples and without any anomalies in any target channel are used for training and validation.
- Only a single output from the LSTM model a single Telemanom model can take multiple input channels but it always outputs a prediction for a single target channel. This is a significant shortcoming when scaling this approach to hundreds of channels and gigabytes of data. The training of a single model may last hours or days, so training separate models for tens of channels can take months on a single PC. Also, it is impossible to provide different sets of input

(non-target channels, telecommands) and output (target) channels. **Telemanom-ESA**: the output of Telemanom is extended, so that is possible to forecast any number of channels at once from a single model, like in DC-VAE[13]. The channels are still analyzed separately, but there is no need to train a separate model for each channel.

• **Problems with GPU support** – the original implementation of Telemanom is based on TensorFlow version 2.0 which does not natively support the CUDA compute capability 8.6 of our Nvidia GPUs. Also, the TimeEval framework lacks GPU support. **Telemanom-ESA**: TensorFlow is upgraded to version 2.5 and the GPU support is added to TimeEval.

#### 3.4.2. GlobalSTD

In this simple distribution-based approach, any samples deviating from the mean of the channel by more than N its standard deviations are detected as anomalies. This approach is categorized as semi-supervised because only nominal samples (excluding annotated events) from the training set are used to compute means and standard deviations for each channel to avoid the influence of outliers. In practice, the threshold of 3 standard deviations (GlobalSTD3) is frequently used (following the empirical statistical rule that 99.7% of data occurs within 3 standard deviations from the mean within a normal distribution [36]), but it may not be optimal when the number of false positives should be minimized, so the threshold of 5 standard deviations (GlobalSTD5) is also tested to provide a versatile baseline for other algorithms. This algorithm is unable to detect local anomalies, so it is not a good choice in practice. It is also not aware of dependencies between channels and it is very vulnerable to changes in the data distribution during the mission. It also cannot use the information about non-target channels and telecommands.

#### 3.4.3. DC-VAE and its adapted version (DC-VAE-ESA)

Dilated Convolutional-Variational Auto Encoder (DC-VAE) [13] is one of the latest published multivariate TSAD algorithms. It is a reconstruction-based method that relies on dilated convolutions to capture long and short-term dependencies without using computation- and memory-intensive multi-layer RNNs. Unlike the original Telemanom, it does not need a complicated thresholding scheme, because it also estimates nominal standard deviations for each sample in each channel, so thresholding can simply be applied by looking for real samples exceeding reconstructions by more than *N* standard deviations. In the original implementation, *N* is selected from integers between 2 and 7 to maximize the range-based F1-score for each channel in the training set. This approach does not scale well with the number of channels and assumes the similarity of anomalies between the training and test sets. Thus, in DC-VAE-ESA, only two values of *N* are considered, 3 (*STD3*) and 5 (*STD5*).

The modified DC-VAE-ESA introduces only two small technical improvements to fully cover 7 of the 9 mentioned requirements, 1) an option to handle different numbers of input and output channels, 2) L2 regularization of convolutional layers with the 0.001 rate to stabilize the training of VAE in the presence of concept drifts.

#### 3.4.4. Experiments with transformers

We have experimented with transformer-based anomaly detectors, namely TranAD [34] and Anomaly Transformer [37] algorithms, using the code from their original repositories. We have not included the results in the current benchmark for several reasons:

- 1. We were not able to achieve any reasonable qualitative results using the default hyperparameters of these algorithms. They would require additional investigation and hyperparameters selection that go beyond the scope of the study and computational resources allocated to it.
- 2. The algorithms are not a part of the TimeEval framework and it would require additional effort to integrate and make them reproducible within our pipeline.
- 3. The original implementations do not handle irregular sampling rates of data. Their data loaders assume uniform sampling when creating windows for training, so it is not possible to take advantage of the positional enconding of transformers.
- 4. The original implementation of Anomaly Transformer provides just a single global anomaly score, so it does not meet the requirement R5 from Table 2 in the main text ("provide a list of affected channels").

Nevertheless, transformers seem to be a promising direction for future work based on the ESA-ADB benchmark.

## 3.4.5. Algorithms' selection

Based on the initial requirements analysis, 20 algorithms were preselected among those available (or added) in the TimeEval framework that at least partially meet all primary requirements. Table 13 summarizes the detailed requirements analysis for those algorithms. Some examples of partially fulfilled requirements are for algorithms that R1) do not provide dedicated thresholding mechanisms, R2) technically allow for the online detection but with a large computational overhead, R4) handle anomalies in training data but cannot learn from them, R5) would need additional mechanisms or modifications of external libraries (i.e., PyOD [38]) to provide a list of affected channels, R7) give only a theoretical option to learn rare nominal events, or R9) are only possible to run for the lightweight subsets of channels (i.e., Windowed iForest and KNN). None of the preselected algorithms are able to explicitly earn rare nominal events (R7) or handle varying sampling rates (R8).

Based on the detailed analysis of the requirements, eight algorithms of various types were selected for ESA-ADB, five unsupervised – principal components classifier (PCC) [39], histogram-based outlier score (HBOS) [40], isolation forest (iForest) [41], k-nearest neighbours (KNN) [42], and three semi-supervised ones – global standard deviations from nominal (GlobalSTD),

Telemanom [5], and DC-VAE [13]. The selected unsupervised algorithms have several important limitations in terms of TSAD. They may be give suboptimal results because of the assumptions of independence of samples and identical fractions of anomalies in training and test data (they fulfil R4 because they learn contamination levels from the training data). They only give global scores, so it is impossible to calculate subsystem-aware and channel-aware scores for them. They also do not support non-target channels and telecommands on input, so this information was not used. However, they establish a baseline for more advanced algorithms.

Among the rejected ones, Matrix Profile-based methods like DAMP [43] or MADRID [44] seem to be promising candidates due to their outstanding speed, high interpretability, and a theoretical possibility to memorize rare nominal events. However, they would need a special adaptation to support multidimensional data [45], they do not give option to annotate known anomalies in training data, and their implementations in Matlab pose several technical and licensing problems when integrated with TimeEval. The COPOD algorithm does not fulfil R9 after adapting it to online detection required by R2. LOF [46], k-Means [47], Torsk [48], and RobustPCA [49] showed very poor results in initial experiments. All semi-supervised algorithms that only partially fulfil R9 were rejected. The published code contains implementations of all methods listed in Table 13.

TABLE 13

ANALYSIS OF PRESELECTED ALGORITHMS ACCORDING TO ESA-ADB REQUIREMENTS. 0/0.5/1 MEANS THAT THE REQUIREMENT IS NOT/PARTIALLY/FULLY FULFILLED. ASTERISKS MARK NEW METHODS ADDED TO THE TIMEEVAL. BOLD-FACED REQUIREMENTS ARE "MUST".

MUSI.											
Algo	orithm	R1	R2	R3	R4	R5	R6	R7	R8	R9	Included in ESA-ADB
	COPOD [50]	1	1	0.5	0.5	1	0	0	0	0.5	NO
	HBOS [40]	1	0	1	0.5	0.5	0	0	0	1	YES
	iForest [41]	1	1	1	0.5	0.5	0	0	0	1	YES
SED	Windowed iForest [41]	1	1	1	0.5	0.5	0	0	0	0.5	SUBSETS
RVI	k-Means [47]	1	1	1	0.5	0.5	0	0	0	0.5	NO
UNSUPERVISED	KNN [42]	1	1	1	0.5	0.5	0	0.5	0	0.5	SUBSETS
SNO	LOF [46]	1	1	1	0.5	0.5	0	0	0	0.5	NO
	Matrix Profile [43], [44]	1	0.5	1	0	0.5	0	0.5	0	1	NO
	PCC [39]	1	1	0.5	0.5	0.5	0	0	0	1	YES
	Torsk [48]	0.5	1	1	0.5	1	0	0	0	0.5	NO
	DAE [51]	0.5	1	1	0	1	0	0	0	0.5	NO
	DC-VAE [13]*	0.5	1	1	0	1	0	0	0	0.5	NO
	DC-VAE-ESA*	1	1	1	0.5	1	1	0	0	1	YES
SEMI-SUPERVISED	GlobalSTD*	1	0	1	0.5	1	0	0	0	1	YES
ERV	Hybrid KNN [52]	1	1	1	0	0.5	0	0.5	0	0.5	NO
SUP	LSTM-AD [53]	0.5	1	1	0	0	0	0	0	0.5	NO
EMI	OmniAnomaly [12]	0.5	1	1	0	0.5	0	0	0	0.5	NO
S	RobustPCA [49]	0.5	1	0.5	0.5	0.5	0	0	0	1	NO
	Telemanom [5]	1	1	1	0	1	0	0	0	0.5	NO
	Telemanom-ESA*	1	1	1	0.5	1	1	0	0	1	YES

## 3.4.6. Algorithms' parametrization

To support the full reproducibility of our results, Table 14 lists all the algorithms' parameters and their values used in our experiments. The parameters' names directly correspond to the published code based on the TimeEval framework [54]. They use default values or settings recommended by algorithms' authors, sometimes adjusted to the specific features of our datasets (boldfaced in the table).

The number of 50 bins in HBOS was arbitrarily selected based on the analysis of the histograms of channels because the default value of 10 seemed to be much too small for our dataset. The default window size in Windowed iForest was decreased

from 100 to 17 to avoid out-of-memory errors for our datasets. Many parameters of DC-VAE were adjusted to our dataset. The scaling is not used because it is already present in our preprocessing. Outliers are not rejected (*wo\_outliers* is False) because our preprocessing code removes known anomalies. The window size is increased to 256 to be similar to the default Telemanom's window size (250). Also, the value of 256 showed good results on similar data in the original DC-VAE paper [13]. The number of CNN units is decreased from the default 64 to 32 because a significant overfitting was noticed in the validation scores for 64 units. The latent space dimensionality depends on the number of input channels in the same way as suggested for the TELCO dataset in the original DC-VAE code. The two main changes to Telemanom are 1) the increased number of units for full set training sets depending on the total number of input and output channels, and 2) the new min\_error\_value parameter to avoid magic numbers in the Telemanom code. The default value of the min\_error\_value is set to 0 (no magic numbers), but for Telemanom-ESA-Pruned it is arbitrarily selected to be 0.007 based on a manual analysis of reconstruction errors for the validation set, since the default value of 0.05 was much too high for some channels.

Importantly, the number of batches per epoch was limited to 1000 to avoid extremely long epoch training times for our datasets and to provide frequent validation score updates. Thus, the number of (sub)epochs was increased tenfold to 1000, and the early stopping patience was doubled to 20 for both DC-VAE and Telemanom to compensate for this.

TABLE 14

PARAMETRIZATION OF ALGORITHMS USED IN ESA-ADB. BOLDFACED PARAMETERS AND VALUES ARE DIFFERENT FROM THE
DEFAULT ONES

	DEFAUI	LT ONES
Algorithm	Parameter name	Value(s)
	max_iter	None
	n_components	None
	n_selected_components	None
PCC	random_state	42
	svd_solver	auto
	tol	0.0
	whiten	False
	n_bins	50
HBOS	alpha	0.1
пвоз	bin_tol	0.5
	random_state	42
	n_trees	100
	bootstrap	False
iForest	max_features	1.0
	max_samples	None
	random_state	42
	n_trees	200
	window_size	17
W' 1 1'E '	bootstrap	False
Windowed iForest	max_features	1.0
	max_samples	None
	random_state	42
	distance_metric_order	2
IZNINI	leaf_size	30
KNN	method	Largest
	n_neighbors	5
CL L ICEP	tol	3 (STD3) and 5 (STD5)
GlobalSTD	random_state	42
	alpha	3 (STD3) and 5 (STD5)
	T (window size)	256
	cnn_units	32 (16 for Phase 1)
	dil_rate	[1,2,4,8,16,32,64]
	kernel	2
	strs (stride length of CNN layers)	1
DC-VAE-ESA	batch_size	64
	J (latent space dimensionality)	1/3 × total number of input channels and telecommands
	epochs	1000
	lr (learning rate)	10-3
	seed	123
	early_stopping_delta	0.001
	early_stopping_patience	20

	batch_size	70
	dropout	0.3
	early_stopping_delta	0.0003
	early_stopping_patience	20
	epochs	1000
	error_buffer	100
	layers	2
		80 for lightweight subsets.
Telemanom-ESA	number of units per layer	Total number of input and output channels for full sets.
	lstm_batch_size	64
	min_error_value (newly introduced	0
	to avoid magic numbers)	(0.007 for Telemanom-ESA-Pruned)
	prediction_window_size	10
	random_state	42
	smoothing_perc	0.05
	smoothing_window_size	30
	window_size	250

## 4. BENCHMARKING RESULTS

TABLE 15

BENCHMARKING RESULTS FOR DETECTION OF ALL EVENTS (EXCLUDING COMMUNICATION GAPS) IN LIGHTWEIGHT SUBSETS OF CHANNELS AND ALL CHANNELS FOR MISSION 1. BOLDFACED RESULTS INDICATE THE BEST VALUES AMONG ALL ALGORITHMS (EXCLUDING AFTER RATIO OF ADTQC WHICH IS JUST A HELPER VALUE).

MISSION	1. BOLDFACE	D RESULTS II	NDICATE THE	BEST VALUE	ES AMONG AL	L ALGORITH	MS (EXCLUDI	NG AFTER R	ATIO OF ADT(	C WHICH IS JU	JST A HELPE	R VALUE).
			M	ission1 – trai	ned and teste	d on the light	tweight subse	t of channels	41-46			
Met	tric	PCC	HBOS	iForest	Window iForest	KNN	Global STD3	Global STD5	DC-VAE- ESA STD3	DC-VAE- ESA STD5	Teleman- ESA	Teleman- ESA-Pruned
	Precision	< 0.001	< 0.001	< 0.001	< 0.001	< 0.001	0.001	0.288	0.002	0.063	0.148	0.999
Event-wise	Recall	0.554	0.585	0.585	0.738	0.754	0.431	0.169	0.554	0.338	0.894	0.424
	F0.5	< 0.001	< 0.001	< 0.001	< 0.001	< 0.001	0.001	0.253	0.003	0.075	0.178	0.786
CI I	Precision		-	-			0.431	0.169	0.550	0.338	0.894	0.424
Channel- aware	Recall	Not available for unsupervised algorithms					0.285	0.159	0.463	0.221	0.738	0.275
awarc	F0.5						0.351	0.167	0.514	0.283	0.837	0.362
Alarm	ing precision	0.033	0.047	0.017	0.015	0.017	0.057	0.035	0.070	0.028	0.868	0.875
ADTQC -	After ratio	0.833	0.763	0.711	0.375	0.612	0.929	0.909	0.972	0.955	0.136	0.143
ADTQC	Score	0.840	0.781	0.784	0.563	0.803	0.770	0.688	0.901	0.803	0.428	0.197
Affiliation-	Precision	0.535	0.543	0.543	0.599	0.522	0.559	0.699	0.584	0.780	0.727	0.711
based	Recall	0.334	0.352	0.357	0.424	0.322	0.375	0.422	0.377	0.593	0.662	0.423
04004	F0.5	0.477	0.490	0.492	0.553	0.464	0.509	0.618	0.526	0.734	0.713	0.626
				Missio	n1 – trained	and tested on	the full set of	f channels				
Met	tric	PCC	HBOS	iForest	Window iForest	KNN	Global STD3	Global STD5	DC-VAE- ESA STD3	DC-VAE- ESA STD5	Teleman- ESA	Teleman- ESA-Pruned
	Precision	< 0.001	< 0.001	< 0.001	11 01000		< 0.001	0.002	< 0.001	0.005	0.007	0.050
Event-wise	Recall	0.870	0.957	0.967			0.848	0.761	0.924	0.804	0.946	0.870
	F0.5	< 0.001	< 0.001	< 0.001			< 0.001	0.003	< 0.001	0.007	0.008	0.061
G. I.	Precision	NT .	1.1.1. 6	. 1			0.520	0.728	0.526	0.640	0.676	0.395
Subsystem- aware	Recall	Not avai	lable for unsugalgorithms	pervised			0.694	0.538	0.764	0.670	0.859	0.861
aware	F0.5		uigoriumis				0.528	0.664	0.538	0.623	0.689	0.436
Ch 1	Precision	N-4:	1-1-1- £		Out-of-	Out-of-	0.380	0.276	0.398	0.359	0.514	0.267
Channel- aware	Recall	Not avai	lable for unsug algorithms	pervised	memory	memory	0.292	0.208	0.414	0.266	0.569	0.725
aware	F0.5		uigomunis				0.325	0.241	0.350	0.282	0.477	0.291
Alarm	ing precision	0.003	0.002	0.001			0.004	0.049	0.002	0.017	0.074	0.206
ADTOC -	After ratio	0.613	0.443	0.438			0.718	0.743	0.647	0.716	0.322	0.463
ADIQC	Score	0.642	0.603	0.685			0.723	0.691	0.752	0.692	0.673	0.684
Affiliation-	Precision	0.563	0.539	0.538			0.560	0.575	0.559	0.578	0.545	0.649
based	Recall	0.522	0.578	0.456			0.492	0.462	0.476	0.511	0.368	0.484
1	F0.5	0.554	0.547	0.519			0.545	0.548	0.540	0.563	0.497	0.607

TABLE 16
BENCHMARKING RESULTS FOR DETECTION OF ALL EVENTS (EXCLUDING COMMUNICATION GAPS) IN LIGHTWEIGHT SUBSETS OF CHANNELS AND ALL CHANNELS FOR MISSION 1. BOLDFACED RESULTS INDICATE THE BEST VALUES AMONG ALL ALGORITHMS (EXCLUDING AFTER RATIO OF ADTQC WHICH IS JUST A HELPER VALUE).

MISSION	NI. BOLDFACE	D RESULTS I								QC WHICH IS I	UST A HELPE	R VALUE).
			N	Iission2 – tra	ined and test	ed on the ligh	itweight subse	t of channels	s 18-28			
Met	tric	PCC	HBOS	iForest	Window iForest	KNN	Global STD3	Global STD5	DC-VAE- ESA STD3	DC-VAE- ESA STD5	Teleman- ESA	Teleman- ESA-Pruned
	Precision	0.029	0.055	0.557	0.951	< 0.001	0.006	0.061	0.003	0.064	0.188	0.978
Event-wise	Recall	1.000	0.911	0.974	0.940	1.000	1.000	1.000	1.000	1.000	0.986	0.540
	F0.5	0.036	0.068	0.609	0.949	0.001	0.007	0.075	0.003	0.079	0.224	0.842
- ·	Precision						0.951	0.992	0.904	0.995	0.831	0.465
Channel- aware	Recall	I	Not available i	for unsupervis	sed algorithms		0.462	0.372	0.554	0.451	0.870	0.384
awaie	F0.5						0.767	0.723	0.787	0.783	0.822	0.442
Alarm	ing precision	0.061	0.105	0.075	0.217	0.060	0.054	0.061	0.052	0.068	0.912	0.862
ADTOC -	After ratio	0.983	0.994	1.000	0.948	0.391	0.946	0.989	0.908	0.991	0.087	0.351
ADTQC	Score	0.999	0.990	0.991	0.985	0.724	0.997	0.997	0.996	0.997	0.507	0.757
Affiliation-	Precision	0.890	0.936	0.982	0.968	0.561	0.740	0.935	0.680	0.939	0.688	0.759
based	Recall	0.580	0.867	0.952	0.925	0.243	0.296	0.717	0.293	0.788	0.544	0.530
ouseu	F0.5	0.804	0.921	0.976	0.959	0.445	0.569	0.881	0.538	0.904	0.654	0.699
				Missi	on2 – trained	and tested or	n the full set o	f channels				
Met	tric	PCC	HBOS	iForest	Window iForest	KNN	Global STD3	Global STD5	DC-VAE- ESA STD3	DC-VAE- ESA STD5	Teleman- ESA	Teleman- ESA-Pruned
	Precision	0.082	0.016	0.022	0.034		0.014	0.203	0.002	0.008	0.052	0.058
Event-wise	Recall	0.983	0.820	0.903	0.746		0.997	0.972	0.997	0.994	0.992	0.964
	F0.5	0.1	0.02	0.027	0.042		0.018	0.241	0.002	0.011	0.064	0.071
Cht	Precision						0.922	0.961	0.672	0.911	0.409	0.258
Subsystem- aware	Recall	Not ava	ailable for uns	upervised algo	orithms		0.953	0.923	0.967	0.952	0.984	0.896
aware	F0.5						0.919	0.946	0.699	0.907	0.451	0.298
Channal	Precision					Out-of-	0.913	0.956	0.774	0.931	0.584	0.326
Channel- aware	Recall	Not ava	ailable for uns	upervised algo	orithms	memory	0.454	0.376	0.592	0.507	0.783	0.823
aware	F0.5						0.745	0.715	0.713	0.783	0.592	0.368
Alarm	ing precision	0.183	0.148	0.112	0.179		0.112	0.179	0.066	0.083	0.771	0.790
Δητος	After ratio	0.980	0.906	0.939	0.852		0.953	0.994	0.663	0.930	0.104	0.274
ADTQC -	Score	0.984	0.939	0.967	0.928	3	0.983	0.992	0.825	0.985	0.513	0.648
715700	Score											
	Precision	0.758	0.570	0.621	0.608		0.718	0.961	0.603	0.859	0.586	0.591
Affiliation- based			0.570 0.455 0.543	0.621 0.499 0.592	0.608 0.474 0.575		0.718 0.385 0.612	0.961 0.833 0.932	0.603 0.324 0.515	0.859 0.625 0.799	0.586 0.348 0.516	0.591 0.347 0.518

#### 4.1. Example detections

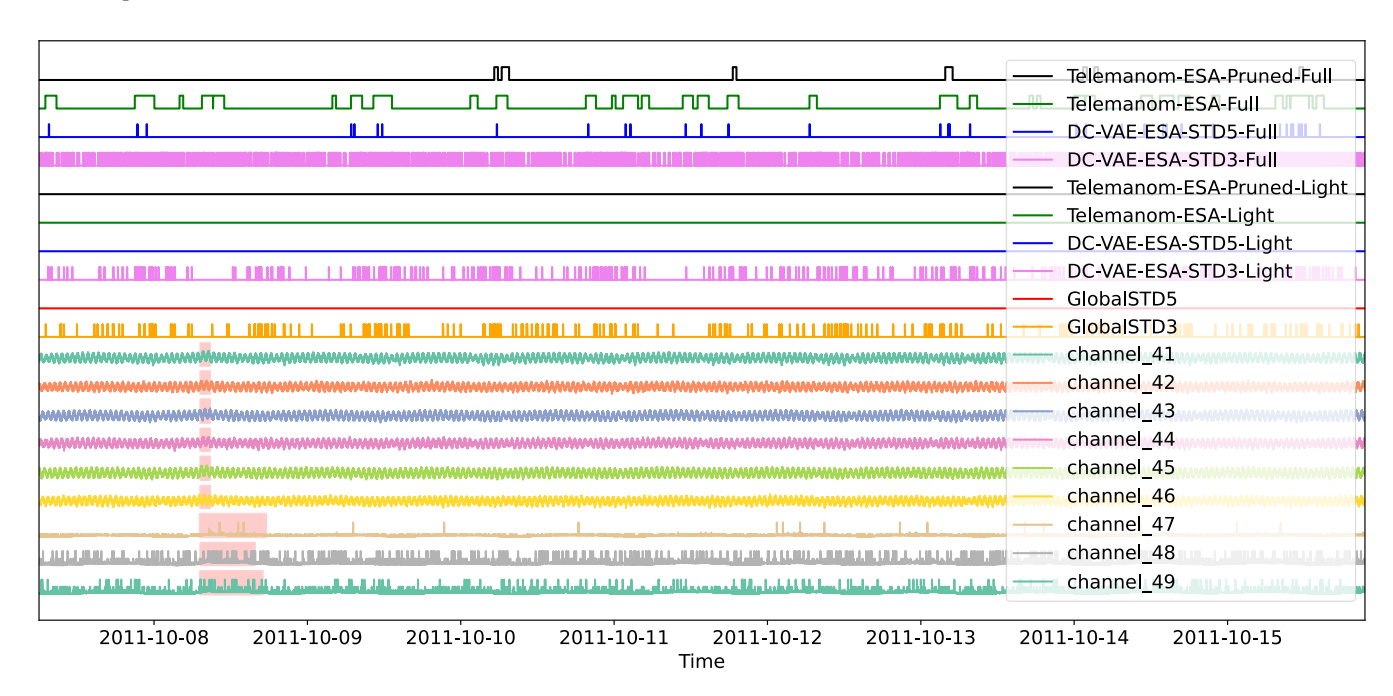


**Fig. 17.** Detections of rare nominal event id\_49 (marked in red) for Mission1. It is not detected when using only the lightweight subset of channels 41-46. For the full set, only Telemanom-ESA shows a reasonable detection, but it is surrounded by many false detections.

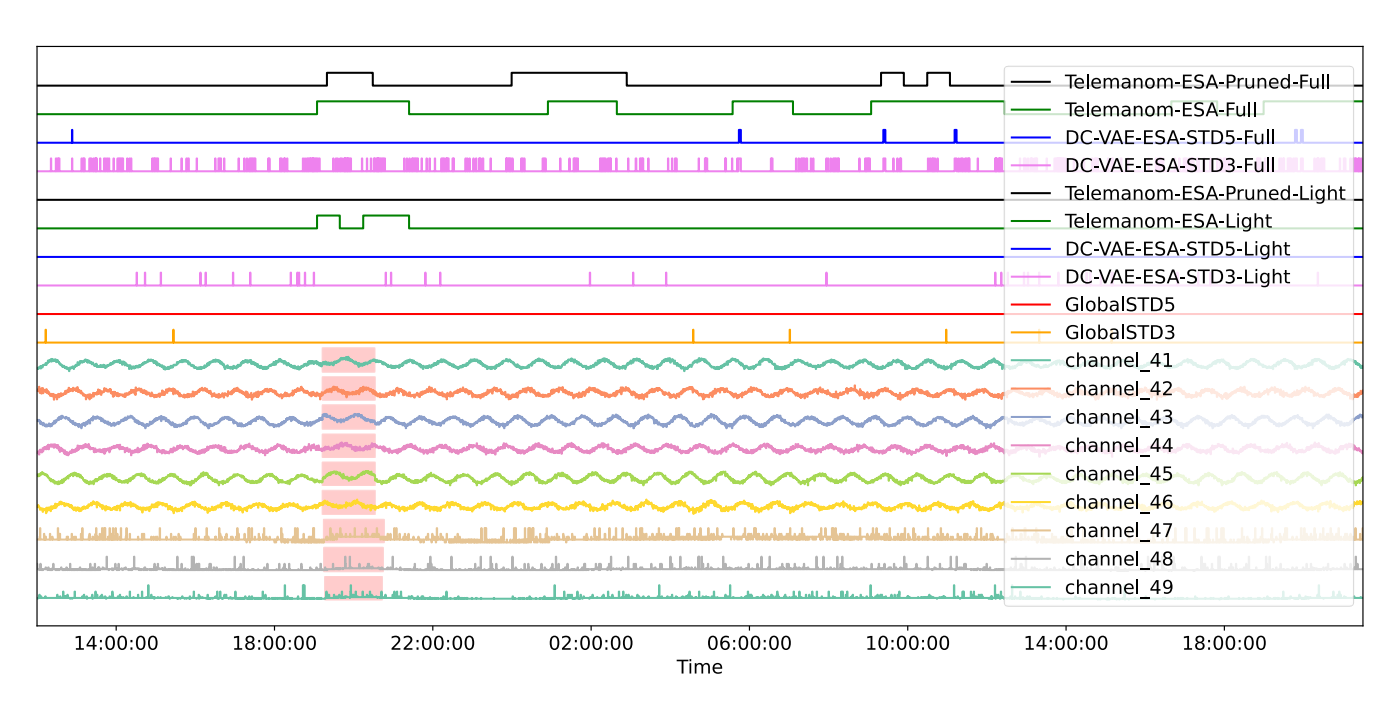


**Fig. 18.** Detections of rare nominal event id\_51 (marked in red) for Mission1. It is reasonably detected only by Telemanom-ESA. Surprisingly, Telemanom-ESA trained on the lightweight subset was also able to detect this.

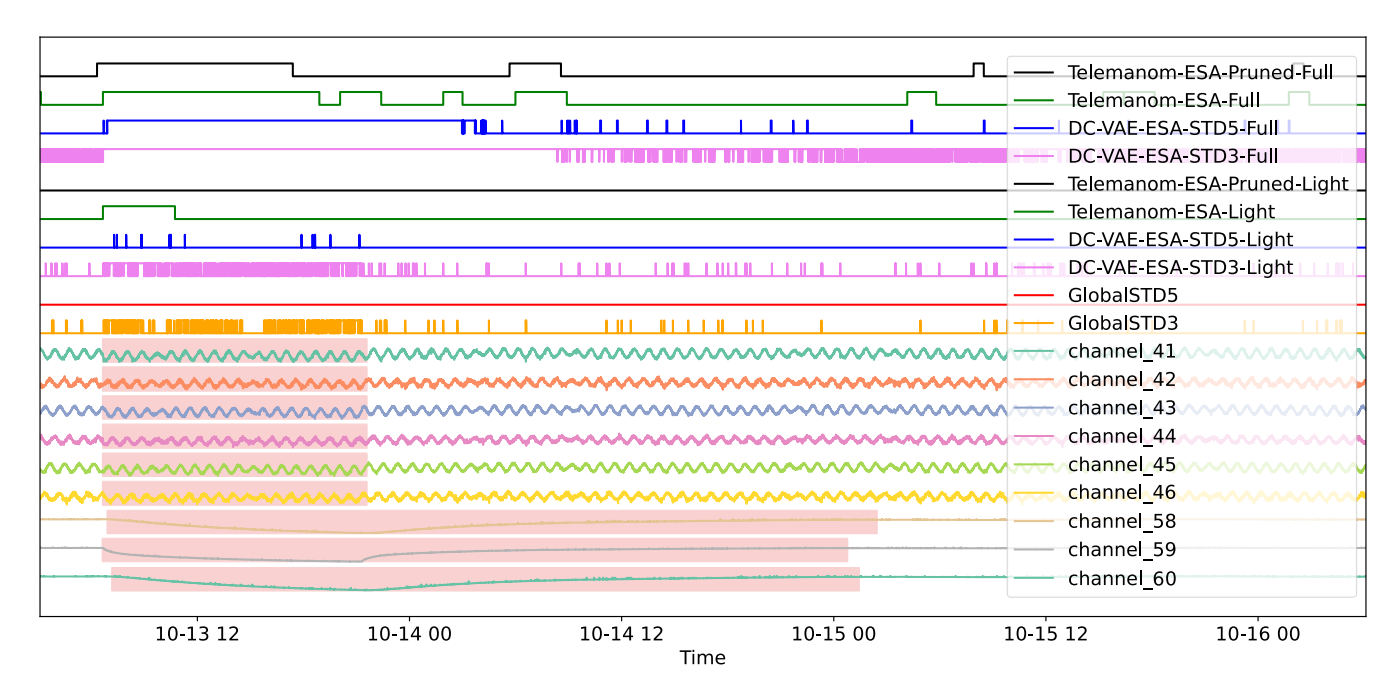


**Fig. 19**. Detections of anomaly id\_138 (marked in red) for Mission1. It is clearly visible in channels 58-60, so it is detected well by models trained on full sets of channels. However, it is not so easy using only the lightweight subset, i.e., Telemanom-ESA-Pruned-Light shows no response.

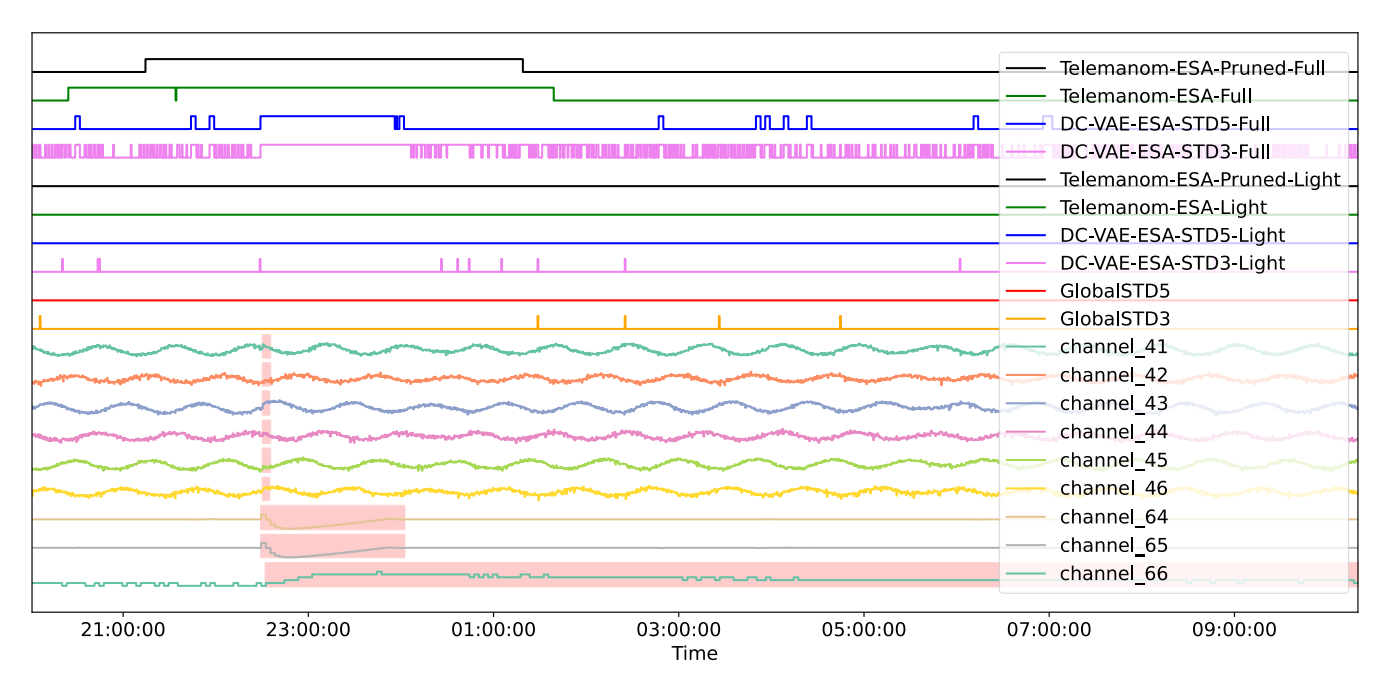


**Fig. 20.** Detections of anomaly id\_153 (marked in red) for Mission1. It is not detected when using only the lightweight subset of channels 41-46. For the full set, it is detected by all algorithms. Telemanom-ESA-Full detects it too early.

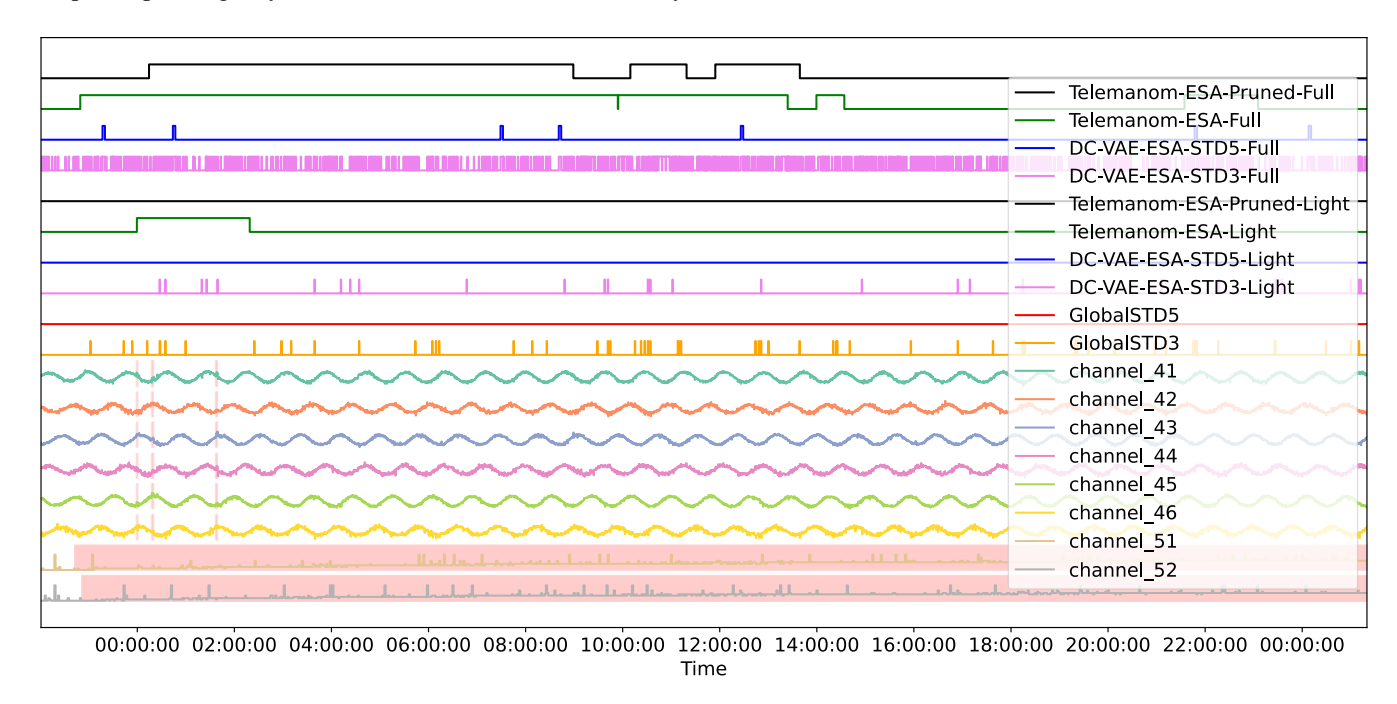
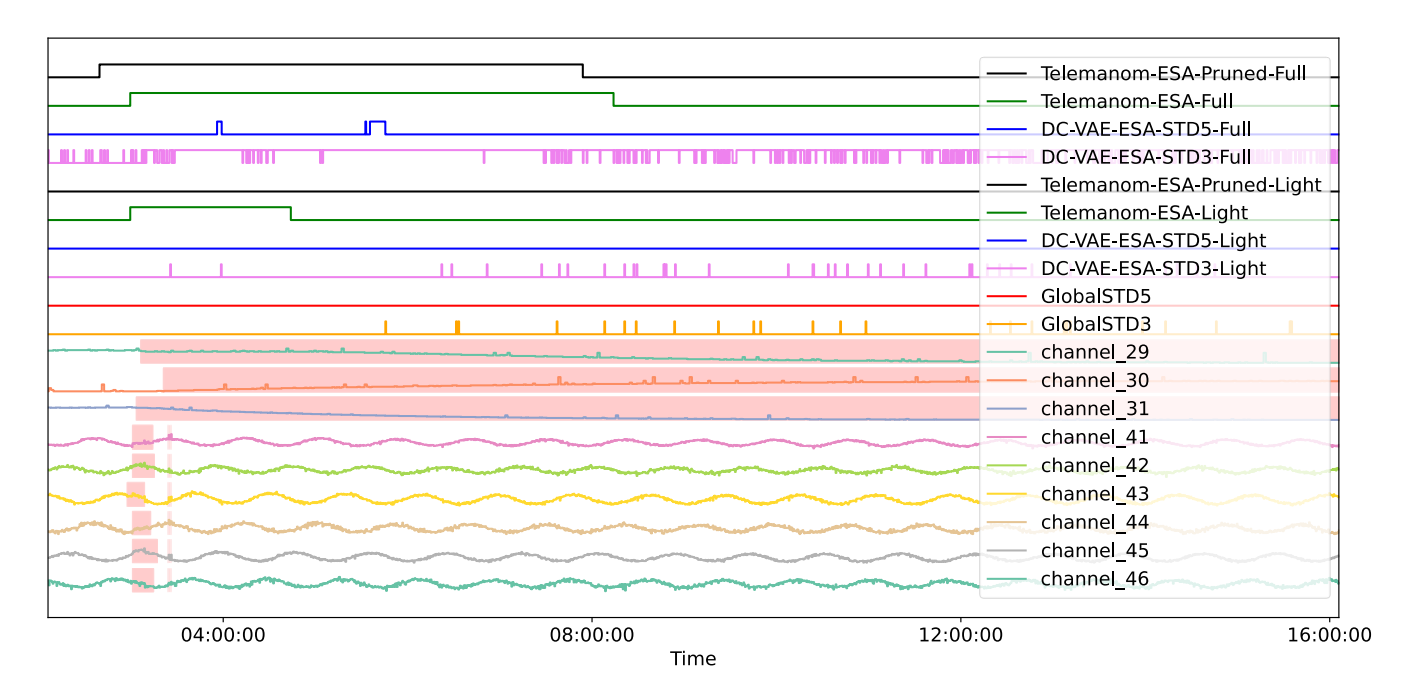
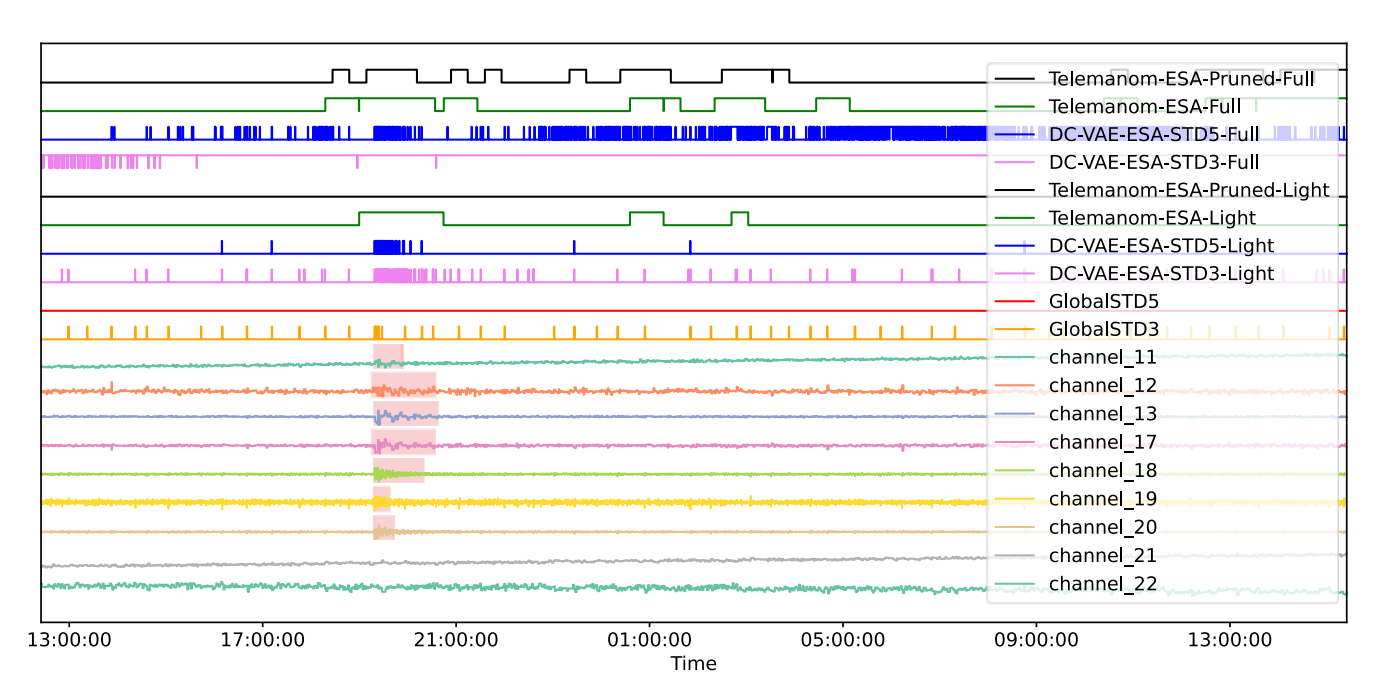


Fig. 21. Detections of rare nominal event id\_155 (marked in red) for Mission1. Only Telemanom-ESA was able to correctly detect this event in both lightweight and full sets of channels.



**Fig. 22.** Detection of rare nominal event id\_159 (marked in red) for Mission1. Only Telemanom-ESA was able to correctly detect this event in both lightweight and full sets of channels, with a good timing. DC-VAE-ESA-STD3-Full also seems to detected it relatively well.



**Fig. 23.** Detection of anomaly id\_631 (marked in red) for Mission2. This anomaly is not so easy to spot manually but was detected by most algorithms, surprisingly, not by Telemanom-ESA-Pruned-Light.

## 4.2. Results for anomalies only

The analysis of the results for anomalies alone (excluding rare nominal events and communication gaps) in Table 17 is important for understanding the performance of the algorithms in detecting the actual anomalies desired by SOEs. In this analysis, any true positives, false positives, or false negatives related to events different than anomalies are ignored (see implementation details in Appendix Section 3.2.2). For Mission2, there are only 9 anomalies in the full test set and only 4 anomalies in the lightweight test set (see Table 21), so the results should be interpreted with caution. A more reliable analysis can be conducted for Mission1 with 55 and 29 anomalies, respectively (see Table 20).

TABLE 17

BENCHMARKING RESULTS FOR DETECTION OF ANOMALIES ONLY IN LIGHTWEIGHT SUBSETS OF CHANNELS AND ALL CHANNELS FOR MISSION 1 IN ESA-ADB. BOLDFACED RESULTS INDICATE THE BEST VALUES AMONG ALL ALGORITHMS (EXCLUDING AFTER RATIO OF ADTQC WHICH IS JUST A HELPER VALUE).

	KESUL13	INDICATE IN				· ·			only anomalies		ek value).	
Met	tric	PCC	HBOS	iForest	Window iForest	KNN	Global STD3	Global STD5	DC-VAE- ESA STD3	DC-VAE- ESA STD5	Teleman- ESA	Teleman- ESA-Pruned
	Precision	< 0.001	< 0.001	< 0.001	< 0.001	< 0.001	< 0.001	0.205	0.001	0.021	0.074	0.999
Event-wise	Recall	0.310	0.379	0.414	0.552	0.448	0.310	0.241	0.310	0.241	0.931	0.862
	F0.5	< 0.001	< 0.001	< 0.001	< 0.001	< 0.001	< 0.001	0.211	0.001	0.026	0.090	0.968
	Precision						0.310	0.241	0.302	0.241	0.931	0.529
Channel-	Recall	1	Not available t	for unsupervis	sed algorithms		0.282	0.241	0.285	0.241	0.882	0.862
aware	F0.5					0.293	0.241	0.297	0.241	0.914	0.722	
Alarm	ing precision	0.102	0.054	0.444	0.889	0.120	0.034	0.024	0.048	0.010	0.818	0.862
ADTOC	After ratio	0.889	0.636	0.500	0.063	0.385	0.889	1.000	1.000	1.000	0.037	0.040
ADTQC -	Score	0.826	0.676	0.730	0.308	0.670	0.826	0.919	0.911	0.921	0.220	0.159
A CC:1:	Precision	0.536	0.543	0.532	0.562	0.521	0.561	0.919	0.559	0.906	0.774	0.927
Affiliation- based	Recall	0.276	0.352	0.294	0.366	0.271	0.335	0.854	0.279	0.850	0.673	0.859
bused	F0.5	0.451	0.490	0.458	0.508	0.440	0.494	0.906	0.466	0.894	0.752	0.912
			N	Iission1 – tra	ined and test	ed on the full	set of channe	els – only and	malies			
Met	tric	PCC	HBOS	iForest	Window iForest	KNN	Global STD3	Global STD5	DC-VAE- ESA STD3	DC-VAE- ESA STD5	Teleman- ESA	Teleman- ESA-Pruned
	Precision	< 0.001	< 0.001	< 0.001			< 0.001	0.001	< 0.001	0.003	0.004	0.032
Event-wise	Recall	0.891	0.964	0.945			0.873	0.818	0.891	0.818	0.945	0.909
	F0.5	< 0.001	< 0.001	< 0.001			< 0.001	0.002	< 0.001	0.004	0.005	0.039
G 1	Precision	3.7	1 1 1 6	. ,			0.491	0.782	0.424	0.648	0.712	0.355
Subsystem- aware	Recall	Not avai	lable for unsug algorithms	pervised			0.721	0.676	0.739	0.721	0.855	0.909
awarc	F0.5		argoriums				0.507	0.748	0.448	0.644	0.717	0.397
CI I	Precision	3.7		. ,	O-4 - f	O-4 -f	0.327	0.355	0.272	0.311	0.497	0.195
Channel- aware	Recall	Not avai	lable for unsur algorithms	pervised	Out-of- memory	Out-of- memory	0.332	0.298	0.398	0.324	0.561	0.705
aware	F0.5		argoriumis		memory	memory	0.309	0.315	0.272	0.291	0.472	0.217
Alarm	ing precision	0.005	0.008	0.005			0.009	0.088	0.003	0.020	0.132	0.278
ADTQC	After ratio	0.633	0.415	0.423			0.708	0.756	0.673	0.733	0.327	0.380
ADIQC	Score	0.611	0.553	0.633			0.728	0.654	0.730	0.654	0.561	0.536
A ffiliation	Precision	0.527	0.512	0.501			0.521	0.531	0.512	0.531	0.512	0.611
Affiliation- based	Recall	0.486	0.563	0.445			0.462	0.434	0.452	0.473	0.344	0.436
based	F0.5	0.519	0.521	0.489			0.508	0.508	0.499	0.518	0.467	0.566

TABLE 18

BENCHMARKING RESULTS FOR DETECTION OF ANOMALIES ONLY IN LIGHTWEIGHT SUBSETS OF CHANNELS AND ALL CHANNELS FOR MISSION 2 IN ESA-ADB. BOLDFACED RESULTS INDICATE THE BEST VALUES AMONG ALL ALGORITHMS (EXCLUDING AFTER RATIO OF ADTOC WHICH IS JUST A HELPER VALUE).

	RESCEISI	TOTOLITE III				· · · · · · · · · · · · · · · · · · ·			_	S JUST A HELPI	ER VALUE).	
			Mission2 -	- trained and	tested on the	iigntweignt	subset of char	ineis 18-28 –	only anomalies	5		
Met	ric	PCC	HBOS	iForest	Window iForest	KNN	Global STD3	Global STD5	DC-VAE- ESA STD3	DC-VAE- ESA STD5	Teleman- ESA	Teleman- ESA-Pruned
	Precision	< 0.001	0.000	0.004	0.000	< 0.001	< 0.001	< 0.001	< 0.001	< 0.001	0.001	0.000
Event-wise	Recall	1.000	0.000	1.000	0.000	1.000	1.000	1.000	1.000	1.000	1.000	0.000
	F0.5	< 0.001	0.000	0.005	0.000	< 0.001	< 0.001	< 0.001	< 0.001	< 0.001	0.001	0.000
a	Precision						1.000	1.000	1.000	1.000	0.600	0.000
Channel- aware	Recall	1	Not available t	or unsupervis	sed algorithms		0.667	0.667	1.000	0.667	1.000	0.000
awarc	F0.5						0.909	0.909	1.000	0.909	0.652	0.000
Alarmi	ing precision	0.032	0.000	0.143	0.000	0.029	0.026	0.036	0.027	0.037	1.000	0.000
ADTQC -	After ratio	1.000	-	1.000	-	1.000	1.000	1.000	1.000	1.000	0.000	-
ADIQC	Score	1.000	-	1.000	-	1.000	1.000	1.000	1.000	1.000	0.358	-
Affiliation-	Precision	0.845	0.500	1.000	0.500	0.705	0.826	0.894	0.816	0.950	0.781	0.500
based	Recall	0.925	0.000	0.971	0.000	0.517	0.862	0.994	0.888	0.981	1.000	0.000
	F0.5	0.860	0.000	0.994	0.000	0.657	0.833	0.912	0.830	0.956	0.817	0.000
			N	lission2 – tra	ined and test	ed on the full	set of channe	ls – only ano	malies			
Met	ric	PCC	HBOS	iForest	Window iForest	KNN	Global	Global	DC-VAE-	DC-VAE-	Teleman-	Teleman-
					Irolest		STD3 I	STD5 I	ESA STD3 1	ESA STD5	ESA I	ESA-Pruned
	Precision	0.001	< 0.001	< 0.001	< 0.001		STD3 < 0.001	STD5 0.001	<b>ESA STD3</b> < 0.001	<b>ESA STD5</b> < 0.001	ESA 0.001	ESA-Pruned 0.001
Event-wise	Precision Recall	<b>0.001</b> 0.667	< 0.001 0.667	< 0.001								
Event-wise					< 0.001		< 0.001	0.001	< 0.001	< 0.001	0.001	0.001
	Recall	0.667	0.667	0.667	< 0.001 0.500		< 0.001 0.667	<b>0.001</b> 0.167	< 0.001 0.833	< 0.001 0.667	0.001 1.000	0.001 1.000
Subsystem-	Recall F0.5	0.667 <b>0.001</b>	0.667	0.667 < 0.001	< 0.001 0.500 < 0.001		< 0.001 0.667 < 0.001	0.001 0.167 0.001	< 0.001 0.833 < 0.001	< 0.001 0.667 < 0.001	0.001 1.000 0.001	0.001 1.000 0.001
	Recall F0.5 Precision	0.667 <b>0.001</b>	0.667 < 0.001	0.667 < 0.001	< 0.001 0.500 < 0.001		< 0.001 0.667 < 0.001 0.167	0.001 0.167 0.001 0.000	< 0.001 0.833 < 0.001 0.333	< 0.001 0.667 < 0.001 0.333	0.001 1.000 0.001 0.417	0.001 1.000 0.001 0.278
Subsystem- aware	Recall F0.5 Precision Recall	0.667 <b>0.001</b>	0.667 < 0.001	0.667 < 0.001	< 0.001 0.500 < 0.001	Out of	< 0.001 0.667 < 0.001 0.167 0.167	0.001 0.167 0.001 0.000 0.000	< 0.001 0.833 < 0.001 0.333 0.500	< 0.001 0.667 < 0.001 0.333 0.333	0.001 1.000 0.001 0.417 0.833	0.001 1.000 0.001 0.278 1.000
Subsystem- aware  Channel-	Recall F0.5 Precision Recall F0.5	0.667 <b>0.001</b> Not ava	0.667 < 0.001	0.667 < 0.001 upervised algo	< 0.001 0.500 < 0.001 orithms	Out-of- memory	< 0.001 0.667 < 0.001 0.167 0.167 0.167	0.001 0.167 0.001 0.000 0.000 0.000	< 0.001 0.833 < 0.001 0.333 0.500 0.352	< 0.001 0.667 < 0.001 0.333 0.333 0.333	0.001 1.000 0.001 0.417 0.833 0.452	0.001 1.000 0.001 0.278 1.000 0.324
Subsystem- aware	Recall F0.5 Precision Recall F0.5 Precision	0.667 <b>0.001</b> Not ava	0.667 < 0.001	0.667 < 0.001 upervised algo	< 0.001 0.500 < 0.001 orithms	Out-of- memory	< 0.001 0.667 < 0.001 0.167 0.167 0.167 0.083	0.001 0.167 0.001 0.000 0.000 0.000 0.000	< 0.001 0.833 < 0.001 0.333 0.500 0.352 0.095	< 0.001 0.667 < 0.001 0.333 0.333 0.333 0.111	0.001 1.000 0.001 0.417 0.833 0.452 0.296	0.001 1.000 0.001 0.278 1.000 0.324 0.082
Subsystem- aware  Channel- aware	Recall F0.5 Precision Recall F0.5 Precision Recall	0.667 <b>0.001</b> Not ava	0.667 < 0.001	0.667 < 0.001 upervised algo	< 0.001 0.500 < 0.001 orithms		< 0.001 0.667 < 0.001 0.167 0.167 0.167 0.083 0.021	0.001 0.167 0.001 0.000 0.000 0.000 0.000 0.000	< 0.001 0.833 < 0.001 0.333 0.500 0.352 0.095 0.229	< 0.001 0.667 < 0.001 0.333 0.333 0.333 0.111 0.042	0.001 1.000 0.001 0.417 0.833 0.452 0.296 0.573	0.001 1.000 0.001 0.278 1.000 0.324 0.082 0.833
Subsystem- aware  Channel- aware  Alarmi	Recall F0.5 Precision Recall F0.5 Precision Recall F0.5 Precision Acter ratio	0.667 0.001 Not ava Not ava 0.364 0.750	0.667 < 0.001 uilable for unsu uilable for unsu 0.308 0.500	0.667 < 0.001 upervised algoupervised algoupervised algoupervised 30.143	< 0.001 0.500 < 0.001 orithms  0.158  0.333		< 0.001 0.667 < 0.001 0.167 0.167 0.083 0.021 0.052 0.031 1.000	0.001 0.167 0.001 0.000 0.000 0.000 0.000 0.000 1.000 1.000	<0.001 0.833 <0.001 0.333 0.500 0.352 0.095 0.229 0.098 0.026 0.600	< 0.001 0.667 < 0.001 0.333 0.333 0.111 0.042 0.083 0.040 0.750	0.001 1.000 0.001 0.417 0.833 0.452 0.296 0.573 0.325 0.375	0.001 1.000 0.001 0.278 1.000 0.324 0.082 0.833 0.096 0.462 0.500
Subsystem- aware  Channel- aware	Recall F0.5 Precision Recall F0.5 Precision Recall F0.5 Precision	0.667 0.001 Not ava Not ava 0.364	0.667 < 0.001 hilable for unsulable for unsu	0.667 < 0.001 upervised algorapervised algorated algorapervised algorated algorapervised algorated al	< 0.001 0.500 < 0.001 orithms  0.158		<0.001 0.667 <0.001 0.167 0.167 0.083 0.021 0.052 0.031	0.001 0.167 0.001 0.000 0.000 0.000 0.000 0.000 0.000 1.000	< 0.001 0.833 < 0.001 0.333 0.500 0.352 0.095 0.229 0.098 0.026	< 0.001 0.667 < 0.001 0.333 0.333 0.311 0.042 0.083 0.040	0.001 1.000 0.001 0.417 0.833 0.452 0.296 0.573 0.325	0.001 1.000 0.001 0.278 1.000 0.324 0.082 0.833 0.096
Subsystem- aware  Channel- aware  Alarmi  ADTQC	Recall F0.5 Precision Recall F0.5 Precision Recall F0.5 Ing precision After ratio Score Precision	0.667 0.001 Not ava Not ava 0.364 0.750 0.542 0.660	0.667 < 0.001 milable for unsurable of the construction of the con	0.667 < 0.001 upervised algo upervised algo 0.143 0.500 0.493 0.618	< 0.001 0.500 < 0.001 orithms  0.158 0.333 0.437 0.616		<0.001 0.667 <0.001 0.167 0.167 0.167 0.083 0.021 0.052 0.031 1.000 0.992 0.523	0.001 0.167 0.001 0.000 0.000 0.000 0.000 0.000 1.000 1.000 0.612 0.500	<0.001 0.833 <0.001 0.333 0.500 0.352 0.095 0.229 0.098 0.026 0.600 0.698 0.539	<0.001 0.667 <0.001 0.333 0.333 0.111 0.042 0.083 0.040 0.750 0.709 0.418	0.001 1.000 0.001 0.417 0.833 0.452 0.296 0.573 0.325 0.375 0.500 0.660	0.001 1.000 0.001 0.278 1.000 0.324 0.082 0.833 0.096 0.462 0.500 0.766 0.620
Subsystem- aware  Channel- aware  Alarmi	Recall F0.5 Precision Recall F0.5 Precision Recall F0.5 Accall F0.5 Ing precision After ratio Score	0.667 0.001 Not ava Not ava 0.364 0.750 0.542	0.667 < 0.001 milable for unsumable for unsu	0.667 < 0.001 upervised algo upervised algo 0.143 0.500 0.493	< 0.001 0.500 < 0.001 orithms  0.158  0.333  0.437		<0.001 0.667 <0.001 0.167 0.167 0.083 0.021 0.052 0.031 1.000 0.992	0.001 0.167 0.001 0.000 0.000 0.000 0.000 0.000 1.000 1.000 0.612	<0.001 0.833 <0.001 0.333 0.500 0.352 0.095 0.229 0.098 0.026 0.600 0.698	<0.001 0.667 <0.001 0.333 0.333 0.111 0.042 0.083 0.040 0.750 0.709	0.001 1.000 0.001 0.417 0.833 0.452 0.296 0.573 0.325 0.375 0.500 0.660	0.001 1.000 0.001 0.278 1.000 0.324 0.082 0.833 0.096 0.462 0.500 0.766

## 4.3. Results for lightweight test sets using algorithms trained on full sets

For algorithms that provide separate anomaly scores for each channel, it is possible to limit the analysis of the global scores to an arbitrary subset of the channels used in training. It is especially useful to directly compare the results between models trained on full sets of channels and models trained only on lightweight subsets. Such a comparison is presented in Table 19 for the DC-VAE-ESA and Telemanom-ESA algorithms. GlobalSTD is omitted because its results do not depend on the number of training channels.

TABLE 19

BENCHMARKING RESULTS FOR DETECTION OF ALL EVENTS IN LIGHTWEIGHT TEST SETS IN ESA-ADB BY ALGORITHMS TRAINED ON LIGHTWEIGHT AND FULL SETS OF CHANNELS. BOLDFACED RESULTS INDICATE THE BETTER VALUE FOR EACH PAIR OF TRAINING SETS FOR EACH ALGORITHM (EXCLUDING AFTER RATIO OF ADTQC WHICH IS JUST A HELPER VALUE)

	TISTOR LACITY				lightweigh			, , , , , , , , , , , , , , , , , , , ,	
Algorithm →		DC-VA	E-ESA	DC-VA	E-ESA	Telema	n ECA	Teleman	n-ESA-
Aigorumi		STI	D3	ST		Telellia		Pruned	
Trained on –	<b>→</b>	Light	Full	Light	Full	Light	Full	Light	Full
	Precision	0.001	0.008	0.014	0.216	0.148	0.027	0.999	0.043
Event-wise	Recall	0.576	0.167	0.318	0.076	0.894	0.439	0.424	0.848
	F0.5	0.001	0.009	0.017	0.158	0.178	0.033	0.786	0.054
Channal	Precision	0.568	0.167	0.318	0.076	0.894	0.439	0.424	0.833
Channel- aware	Recall	0.442	0.101	0.207	0.066	0.738	0.328	0.275	0.848
awarc	F0.5	0.506	0.134	0.262	0.071	0.837	0.377	0.362	0.834
Alarmi	ing precision	0.052	0.072	0.034	0.119	0.868	0.659	0.875	0.505
ADTQC	After ratio	0.921	0.909	0.952	0.800	0.136	0.586	0.143	0.286
ADTQC	Score	0.805	0.607	0.799	0.728	0.428	0.625	0.197	0.431
Affiliation-	Precision	0.577	0.562	0.741	0.524	0.727	0.616	0.711	0.621
based	Recall	0.373	0.238	0.555	0.071	0.662	0.400	0.423	0.512
bused	F0.5	0.520	0.441	0.694	0.231	0.713	0.556	0.626	0.596
					lightweigh	t test set			
Algorithm →		DC-VA		DC-VAE-ESA		Teleman-ESA		Teleman-ESA- Pruned	
Trained on –		STI Light	Full	STD5  Light Full		T : mln4	Full	Light	nea Full
Trained on –	Precision	0.003	0.003	0.064	0.017	Light <b>0.188</b>	0.152	0.978	0.268
Event-wise	Recall	1.000	1.000	1.000	1.000	0.986	0.132	0.540	0.200
Lvent wise	F0.5	0.003	0.004	0.079	0.021	0.224	0.183	0.842	0.312
	Precision	0.904	0.912	0.995	0.985	0.831	0.875	0.465	0.690
Channel-	Recall	0.554	0.543	0.451	0.445	0.870	0.739	0.384	0.848
aware	F0.5	0.787	0.788	0.783	0.772	0.822	0.823	0.442	0.708
Alarming pre	ecision	0.052	0.034	0.068	0.046	0.912	0.907	0.862	0.861
	After ratio	0.908	0.848	0.991	0.966	0.087	0.105	0.351	0.350
ADTQC	Score	0.996	0.934	0.997	0.989	0.507	0.508	0.757	0.676
A CC:1: - 4'	Precision	0.680	0.675	0.939	0.914	0.688	0.681	0.759	0.738
Affiliation- based	Recall	0.293	0.345	0.788	0.782	0.544	0.503	0.530	0.623
vaseu	F0.5	0.538	0.566	0.904	0.884	0.654	0.636	0.699	0.712

#### 4.4. Results for different mission phases

It is a common practice to periodically retrain or adapt algorithms when new telemetry becomes available from satellites, especially in the presence of significant changes in operational conditions. The experiments in this section simulate such an approach in ESA-ADB to assess the robustness of algorithms to changing conditions and to identify the earliest mission phase in which reliable detectors can be trained. These aspects are crucial for the selection of algorithms in different mission phases. Some classic algorithms may perform much better than others in early mission phases when very limited data is available, but they may be overcome by deep learning techniques in late mission phases. The goal of this section is to provide a basic analysis of these aspects in ESA-ADB. For this purpose, the effect of training set size (representing different mission phases) on the corrected event-wise F0.5-score for the test set is analyzed for the lightweight subsets of each. The analysis for full sets is not conducted as the scores are very low even for the longest training set. There are 5 training set lengths (phases) proposed for Mission1 and 4 for Mission2 following the idea presented in Fig. 24. Starting from just a few percent of the mission timeline (initial phases) to 50% of the mission (the default setting in ESA-ADB). The statistics of the phases are listed in Table 20 (Mission1) and Table 21 (Mission2).

As visualized in Table 22, there is a clear correlation between the training set length and the event-wise F0.5 scores for test sets for both missions. Especially significant improvements are visible between phases 2 and 3 for Mission1 and phases 1 and 2 for Mission 2. A clear example is Windowed iForest for which the event-wise F0.5-score goes from 0.020 to 0.901 for Mission2 in the phase 2. Based on this observation, the minimal reasonable training length can be estimated to be 21 months for Mission1 and 5 months for Mission2. Surprisingly, the longest training sets do not always ensure the best results. There are some exceptions for which training on the longest training set does not give optimal results, i.e., PCC, DC-VAE-ESA, and Telemanom-ESA. We can only hypothesize what is the reason behind that, but it may be related to the concept drift present in the data.

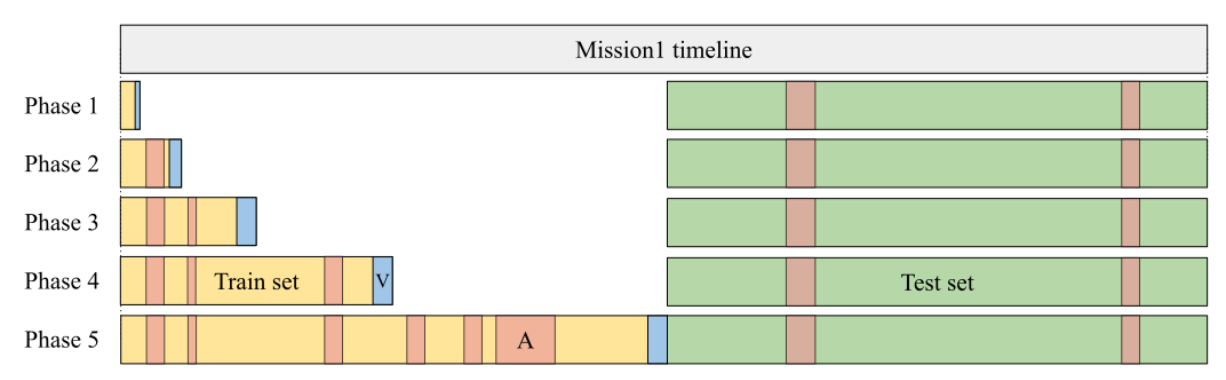


Fig. 24. Illustration of the idea of mission phases for Mission1. "A" marks light red anomalous fragments and "V" marks blue validation fragments.

TABLE 20
STATISTICS OF TRAINING, VALIDATION, AND TEST SETS FOR DIFFERENT PHASES OF MISSION1 CONSIDERING THE FULL SET (TOP PANEL) AND THE LIGHTWEIGHT SUBSET OF CHANNELS (BOTTOM PANEL)

Mission1 – the	Phas	se 1	Phas		Pha	,	Pha	se 4	Pha	se 5	Test
lightweight subset	Train	Val	Train	Val	Train	Val	Train	Val	Train	Val	
Data points	1,125,600	314,399	3,900,977	997,530	8,900,105	1,479,360	19,171,279	1,463,274	39,774,080	1,479,370	40,925,288
Telecommands' executions	7,769	15,918	94,426	45,194	271,882	13,295	414,927	9,001	764,648	60,157	769,917
Duration (anonymised)	9 weeks	3 weeks	8 months	2 months	18 months	3 months	39 months	3 months	81 months	3 months	84 months
Annotated points [%]	1.41	17.29	2.76	1.49	3.24	0.02	1.84	0.11	1.74	1.23	1.81
Annotated events	1	1	6	3	17	2	28	1	52	3	65
Anomalies	0	1	3	1	5	0	10	0	22	2	29
Rare nominal events	1	0	3	2	9	2	14	1	26	1	36
Communication gaps	0	0	0	0	3	0	4	0	4	0	0
Univariate / Multivariate	0 / 1	0 / 1	0/6	0/3	0 / 14	0/2	0 / 24	0 / 1	0 / 48	0/3	1 / 64
Global / Local	1/0	1/0	4 / 2	2 / 1	11/3	1 / 1	18 / 6	1/0	39 / 9	3/0	40 / 25
Point / Subsequence	0 / 1	0 / 1	0/6	0/3	0 / 14	0/2	0 / 24	0 / 1	1 / 47	2 / 1	9 / 56
Distinct event classes	1	1	5	2	10	2	15	1	17	2	13
Mission1 - the full set	Pha	se 1	Pha	se 2	Pha	se 3	Pha	se 4	Pha	se 5	Test
Mission1 - the full set	Phas Train	se 1	Pha: Train	se 2 Val	Pha: Train	se 3	Pha Train	se 4 Val	Pha Train	se 5	Test
Mission1 - the full set  Data points											Test 428,599,738
	Train	Val	Train	Val	Train	Val	Train	Val	Train	Val	
Data points	Train 8,954,221	Val 2,176,171	Train 29,416,435	Val 7,890,008	Train 68,888,013	Val 10,761,293	Train 144,775,815	Val 10,273,971	Train 305,515,601	Val 10,741,556	428,599,738
Data points Annotated points [%]	Train 8,954,221 2.11	Val 2,176,171 10.62	Train 29,416,435 1.87	Val 7,890,008	Train 68,888,013 1.96	Val 10,761,293 0.93	Train 144,775,815 1.32	Val 10,273,971 0.03	Train 305,515,601 1.33	Val 10,741,556	<b>428,599,738</b> 2.25
Data points Annotated points [%] Annotated events	Train 8,954,221 2.11 5	Val 2,176,171 10.62 4	Train 29,416,435 1.87 20	Val 7,890,008 1.52 8	Train 68,888,013 1.96 54	Val 10,761,293 0.93 4	Train 144,775,815 1.32 73	Val 10,273,971 0.03	Train 305,515,601 1.33 104	Val 10,741,556 1.62 5	428,599,738 2.25 91
Data points Annotated points [%] Annotated events Anomalies	Train 8,954,221 2.11 5	Val 2,176,171 10.62 4	Train 29,416,435 1.87 20 13	Val 7,890,008 1.52 8	Train 68,888,013 1.96 54 27	Val 10,761,293 0.93 4 2	Train 144,775,815 1.32 73 40	Val 10,273,971 0.03 1	Train 305,515,601 1.33 104 59	Val 10,741,556 1.62 5	428,599,738  2.25  91  55
Data points  Annotated points [%]  Annotated events  Anomalies  Rare nominal events	Train 8,954,221 2.11 5 4	Val 2,176,171 10.62 4 1 3	Train 29,416,435 1.87 20 13 7	Val 7,890,008 1.52 8 2 6	Train 68,888,013 1.96 54 27 24	Val 10,761,293 0.93 4 2 2	Train 144,775,815 1.32 73 40 29	Val 10,273,971 0.03 1 0 1	Train 305,515,601 1.33 104 59 41	Val 10,741,556 1.62 5 4	428,599,738  2.25  91  55  36
Data points  Annotated points [%]  Annotated events  Anomalies  Rare nominal events  Communication gaps	Train 8,954,221 2.11 5 4 1 0	Val 2,176,171 10.62 4 1 3 0	Train 29,416,435 1.87 20 13 7 0	Val 7,890,008 1.52 8 2 6 0	Train 68,888,013 1.96 54 27 24 3	Val 10,761,293 0.93 4 2 2 0	Train 144,775,815 1.32 73 40 29	Val 10,273,971 0.03 1 0 1 0	Train 305,515,601 1.33 104 59 41 4	Val 10,741,556 1.62 5 4 1	428,599,738  2.25  91  55  36  0
Data points  Annotated points [%]  Annotated events  Anomalies  Rare nominal events  Communication gaps  Univariate / Multivariate	Train 8,954,221 2.11 5 4 1 0 3/2	Val 2,176,171 10.62 4 1 3 0 3 / 1	Train 29,416,435 1.87 20 13 7 0 11/9	Val 7,890,008 1.52 8 2 6 0 5/3	Train 68,888,013 1.96 54 27 24 3 31/20	Val 10,761,293 0.93 4 2 2 0 0/4	Train 144,775,815 1.32 73 40 29 4 31/38	Val 10,273,971 0.03 1 0 1 0 0 1 0 1 0 1 0 1 0 1	Train 305,515,601 1.33 104 59 41 4 31/69	Val 10,741,556 1.62 5 4 1 0 0/5	428,599,738  2.25  91  55  36  0  1/90

TABLE 21

STATISTICS OF TRAINING, VALIDATION, AND TEST SETS FOR DIFFERENT PHASES OF MISSION2 CONSIDERING THE FULL SET (TOP PANEL) AND THE LIGHTWEIGHT SUBSET OF CHANNELS (BOTTOM PANEL). THERE ARE NO COMMUNICATION GAPS AND ALL EVENTS ARE OF SUBSEQUENCE TYPE, SO THESE STATISTICS ARE OMITTED.

Mission2 – the	Pha	se 1	Pha	se 2	Pha	se 3	Pha	se 4	Test
lightweight subset	Train	Val	Train	Val	Train	Val	Train	Val	
Data points	1,457,269	506,869	7,741,250	2,032,657	15,714,523	3,867,017	34,998,975	5,830,297	46,153,954
Telecommands' executions	34,185	11,694	179,930	48,313	372,643	93,496	815,370	130,968	1,077,677
Duration (anonymised)	3 weeks	1 week	4 months	1 month	8 months	2 months	18 months	3 months	21 months
Annotated points [%]	0.83	0.49	2.62	2.02	1.94	3.10	3.74	1.02	2.02
Annotated events	14	4	83	19	140	27	246	27	349
Anomalies	0	0	2	2	11	2	18	0	4
Rare nominal events	14	4	81	17	129	25	228	27	345
Univariate / Multivariate	0 / 14	0 / 4	0 / 83	0 / 19	0 / 140	0 / 27	1 / 245	0 / 27	1 / 348
Global / Local	12 / 2	3 / 1	67 / 16	17 / 2	119 / 21	24 / 3	214 / 32	26 / 1	333 / 16
	_	_							
Distinct event classes	3	3	12	6	15	9	21	5	22
Distinct event classes  Mission2 – the full set	Pha		Pha		15 Pha			se 4	Test
	Pha	se 1	Pha	se 2	Pha	se 3	Pha	se 4	
Mission2 – the full set	Pha Train	se 1	Pha Train	se 2	Pha Train	se 3	Pha Train	se 4	Test
Mission2 – the full set  Data points	Pha Train 13,914,918	val 4,841,396	Pha Train 74,356,579	se 2 Val 19,067,743	Pha Train 151,093,710	se 3 Val 37,624,768	Pha Train 338,658,318	se 4 Val 56,746,734	Test 444,603,954
Mission2 – the full set  Data points  Annotated points [%]	Pha Train 13,914,918 0.20	val 4,841,396 0.12	Pha Train 74,356,579 0.64	Val 19,067,743 0.51	Pha Train 151,093,710 0.50	val 37,624,768 0.59	Pha Train 338,658,318 0.66	se 4 Val 56,746,734 0.21	Test 444,603,954 0.54
Mission2 – the full set  Data points  Annotated points [%]  Annotated events	Pha Train 13,914,918 0.20 14	Val 4,841,396 0.12	Pha Train 74,356,579 0.64 85	Val 19,067,743 0.51 22	Pha Train 151,093,710 0.50 146	se 3  Val  37,624,768  0.59  28	Pha Train 338,658,318 0.66 256	se 4  Val  56,746,734  0.21  27	Test 444,603,954 0.54 361
Mission2 – the full set  Data points  Annotated points [%]  Annotated events  Anomalies	Pha Train 13,914,918 0.20 14	se 1 Val 4,841,396 0.12 4	Pha Train 74,356,579 0.64 85	se 2 Val 19,067,743 0.51 22 5	Pha Train 151,093,710 0.50 146	se 3  Val  37,624,768  0.59  28	Pha Train 338,658,318 0.66 256 25	se 4  Val  56,746,734  0.21  27	Test  444,603,954  0.54  361  9
Mission2 – the full set  Data points  Annotated points [%]  Annotated events  Anomalies  Rare nominal events	Pha Train 13,914,918 0.20 14 0 14	val 4,841,396 0.12 4 0 4	Pha Train 74,356,579 0.64 85 4 81	val 19,067,743 0.51 22 5	Pha Train 151,093,710 0.50 146 16 130	se 3  Val  37,624,768  0.59  28  3  25	Pha Train 338,658,318 0.66 256 25 231	se 4  Val  56,746,734  0.21  27  0  27	Test  444,603,954  0.54  361  9  352

TABLE 22

THE EFFECT OF MISSION PHASE ON THE CORRECTED EVENT-WISE F0.5-SCORE FOR SELECTED ALGORITHMS TRAINED AND TESTED ON THE LIGHTWEIGHT SUBSETS OF CHANNELS FROM MISSIONS IN ESA-ADB. BOLDFACED RESULTS INDICATE THE BEST VALUES AMONG ALL PHASES.

FROM MISSIONS IN ESA-ADD. DOEDFACED RESULTS INDICATE THE BEST VALUES AMONG ALL HIASES.												
	Mission1 – trained and tested on lightweight subset of channels 41-46											
Dhasa	DCC	IIDOG	:Eamart	Window	IZNINI	Global	Global	DC-VAE-	DC-VAE-	Teleman-	Teleman-	
Phase	PCC	HBOS	iForest	iForest	KNN	STD3	STD5	ESA STD3	ESA STD5	ESA	ESA-Pruned	
1							0.041	۰ 0 001	0.007	0.059	0.227	
2						c 0 001	0.037	< 0.001	0.012	0.058	0.311	
3			< 0.001			< 0.001	0.104	0.007	0.085	0.122	0.776	
4							0.217	0.009	0.030	0.309	0.776	
5						0.001	0.253	0.003	0.075	0.178	0.786	
				Mission2 – tra	ained and test	ed on lightweig	ght subset of cl	hannels 18-28				
Dhasa	DCC	IIDOG	:Eamart	Window	IZNINI	Global	Global	DC-VAE-	DC-VAE-	Teleman-	Teleman-	
Phase	PCC	HBOS	iForest	iForest	KNN	STD3	STD5	ESA STD3	ESA STD5	ESA	ESA-Pruned	
1	< 0.001	< 0.001	0.006	0.020		< 0.001	< 0.001	۰ 0 001	< 0.001	0.234	0.622	
2	0.062	0.007	0.456	0.901	< 0.001	0.001	0.011	< 0.001	0.001	0.259	0.757	
3	0.013	0.040	0.585	0.947		0.006	0.014	0.001	0.009	0.253	0.731	
4	0.036	0.068	0.609	0.949	0.001	0.007	0.075	0.003	0.079	0.224	0.842	

#### 4.5. Computational resources and limitations

Experiments were run on three different machines:

- 1. Nvidia Tesla T4 GPU (16 GB VRAM), Intel Xeon Gold 5222 CPU 3.80 GHz, and 64 GB RAM, (for CPU-intensive and memory-intensive algorithms)
- 2. Nvidia 3060 RTX GPU (6 GB VRAM), Intel i7-10870H CPU 2.20 GHz, and 32 GB RAM
- 3. Nvidia 3090 RTX GPU (24 GB VRAM), Intel i7-8700H CPU 3.20 GHz, and 32 GB RAM (for GPU-intensive algorithms)

Given the limited resources, there are limits to the amount of time and memory that each algorithm can run. The algorithm is rejected with an *out-of-memory error* if Machine 1 goes out of RAM. Algorithms are rejected with an *out-of-time error* if it takes more than 5 days to train or test a CPU-intensive algorithm on Machine 1, or a GPU-intensive algorithm on Machine 3.

#### 4.6. Processing times

Algorithms for satellite telemetry monitoring must not only be accurate but also fast enough to run in real-time on computational resources available to mission control and, in the extreme case, on board satellites. We measured the times of training (Table 23) and execution (Table 24) of algorithms on our hardware resources (listed in Appendix Section 4.5). These numbers are not directly comparable because the algorithms were run in parallel processes on different machines. They give a rough approximation of the computational burden of each algorithm based on a single run in ESA-ADB. The training and execution times do not include resampling which was done once as an intermediate step before all experiments. The resampling of the test sets took about 1.5 hours for Mission1 and around 1 hour for Mission2, both on Machine 2.

The deep learning-based Telemanom has the longest training and execution times (excluding the execution time of KNN for channels 18-28 of Mission2), but it is still fast enough to provide real-time anomaly detection in both missions using the proposed resampling (0.033 Hz for Mission1, 0.056 Hz for Mission2). The total execution time (including resampling) for the full Mission1 test set is 3.5h which is just 0.02% of the test set duration, for Mission2 it is 4.5h and 0.08%, respectively. Thus, real-time execution should be possible even for sampling rates higher than 30 Hz. Moreover, in our previous works, we have shown that Telemanom can be run in real-time on-board the OPS-SAT satellite with a limited number of channels [55]. The important advantage of simple algorithms is that they are very fast and their training and execution times do not grow significantly with the number of channels, so it may be feasible to retrain them frequently during a mission.

TABLE 23
TRAINING TIMES (IN SECONDS) OF ALGORITHMS USED IN ESA-ADB

Alaanithm	Mission1	train set	Mission2 train set			
Algorithm	channels 41-46	Full	channels 18-28	Full		
PCC	90	143	63	75		
HBOS	110	111	66	68		
iForest	655	714	345	308		
Windowed iForest	2833 (0.8h)	Out-of-memory	1998 (0.6h)	14585 (4h)		
KNN	3844 (1h)	Out-of-memory	4754 (1.5h)	Out-of-memory		
GlobalSTD	101	108	60	90		
DC-VAE-ESA	13466 (3.7h)	18210 (5h)	12440 (3.5h)	4679 (1.3h)		
Telemanom-ESA	13115 (3.6h)	30451 (8.5h)	19725 (5.5h)	12328 (3.5h)		

TABLE 24
EXECUTION TIMES (IN SECONDS) OF ALGORITHMS USED IN ESA-ADB

Alaamithaa	Mission	1 test set	Mission2 test set			
Algorithm	channels 41-46	Full	channels 18-28	Full		
PCC	124	141	73	76		
HBOS	135	137	74	76		
iForest	393	369	199	174		
Windowed iForest	586	Out-of-memory	381	939		
KNN	1233	Out-of-memory	21673 (6h)	Out-of-memory		
GlobalSTD	178	182	95	289		
DC-VAE-ESA	5251 (1.5h)	6010 (1.7h)	3068 (0.9h)	7900 (2.2h)		
Telemanom-ESA	6931 (1.9h)	7271 (2h)	4666 (1.3h)	11078 (3.1h)		

#### 4. References

- [1] A. Blázquez-García, A. Conde, U. Mori, and J. A. Lozano, "A Review on Outlier/Anomaly Detection in Time Series Data," *ACM Comput. Surv.*, vol. 54, no. 3, p. 56:1-56:33, Apr. 2021, doi: 10.1145/3444690.
- [2] K.-H. Lai, D. Zha, J. Xu, Y. Zhao, G. Wang, and X. Hu, "Revisiting Time Series Outlier Detection: Definitions and Benchmarks," in *Proceedings of the Neural Information Processing Systems Track on Datasets and Benchmarks*, Virtual Event, Jan. 2022. Accessed: Oct. 12, 2022. [Online]. Available: https://openreview.net/forum?id=r8IvOsnHchr
- [3] D. Lakey and T. Schlippe, "A Comparison of Deep Learning Architectures for Spacecraft Anomaly Detection," in 2024 IEEE Aerospace Conference, Mar. 2024, pp. 1–11. doi: 10.1109/AERO58975.2024.10521015.
- [4] R. Wu and E. Keogh, "Current Time Series Anomaly Detection Benchmarks are Flawed and are Creating the Illusion of Progress," *IEEE Trans. Knowl. Data Eng.*, vol. 35, no. 3, pp. 2421–2429, Mar. 2023, doi: 10.1109/TKDE.2021.3112126.
- [5] K. Hundman, V. Constantinou, C. Laporte, I. Colwell, and T. Soderstrom, "Detecting Spacecraft Anomalies Using LSTMs and Nonparametric Dynamic Thresholding," in *Proceedings of the 24th ACM SIGKDD International Conference on Knowledge Discovery & Data Mining*, Jul. 2018, pp. 387–395. doi: 10.1145/3219819.3219845.
- [6] D. Wagner, T. Michels, F. C. F. Schulz, A. Nair, M. Rudolph, and M. Kloft, "TimeSeAD: Benchmarking Deep Multivariate Time-Series Anomaly Detection," *Trans. Mach. Learn. Res.*, Apr. 2023, Accessed: Aug. 22, 2023. [Online]. Available: https://openreview.net/forum?id=iMmsCI0JsS
- [7] M. Amin Maleki Sadr, Y. Zhu, and P. Hu, "An Anomaly Detection Method for Satellites Using Monte Carlo Dropout," *IEEE Trans. Aerosp. Electron. Syst.*, vol. 59, no. 2, pp. 2044–2052, Apr. 2023, doi: 10.1109/TAES.2022.3206257.
- [8] F. Sanchez, C. Pankratz, D. M. Lindholm, R. Christofferson, D. Osborne, and T. Baltzer, "WebTCAD: A Tool for Ad-hoc Visualization and Analysis of Telemetry Data for Multiple Missions," in 2018 SpaceOps Conference, Marseille, France: American Institute of Aeronautics and Astronautics, May 2018. doi: 10.2514/6.2018-2616.
- [9] M. Petković *et al.*, "Machine-learning ready data on the thermal power consumption of the Mars Express Spacecraft," *Sci. Data*, vol. 9, no. 1, p. 229, May 2022, doi: 10.1038/s41597-022-01336-z.
- [10] A. P. Mathur and N. O. Tippenhauer, "SWaT: a water treatment testbed for research and training on ICS security," in 2016 International Workshop on Cyber-physical Systems for Smart Water Networks (CySWater), Apr. 2016, pp. 31–36. doi: 10.1109/CySWater.2016.7469060.
- [11] C. M. Ahmed, V. R. Palleti, and A. P. Mathur, "WADI: a water distribution testbed for research in the design of secure cyber physical systems," in *Proceedings of the 3rd International Workshop on Cyber-Physical Systems for Smart Water Networks*, in CySWATER '17. New York, NY, USA: Association for Computing Machinery, Kwiecie 2017, pp. 25–28. doi: 10.1145/3055366.3055375.
- [12] Y. Su, Y. Zhao, C. Niu, R. Liu, W. Sun, and D. Pei, "Robust Anomaly Detection for Multivariate Time Series through Stochastic Recurrent Neural Network," in *Proceedings of the 25th ACM SIGKDD International Conference on Knowledge Discovery & Data Mining*, in KDD '19. New York, NY, USA: Association for Computing Machinery, Jul. 2019, pp. 2828–2837. doi: 10.1145/3292500.3330672.
- [13] G. G. González, S. M. Tagliafico, A. Fernández, G. Gómez, J. Acuna, and P. Casas, "One Model to Find Them All Deep Learning for Multivariate Time-Series Anomaly Detection in Mobile Network Data," *IEEE Trans. Netw. Serv. Manag.*, 2023, doi: 10.1109/TNSM.2023.3340146.
- [14] V. Jacob, F. Song, A. Stiegler, B. Rad, Y. Diao, and N. Tatbul, "Exathlon: a benchmark for explainable anomaly detection over time series," *Proc. VLDB Endow.*, vol. 14, no. 11, pp. 2613–2626, Oct. 2021, doi: 10.14778/3476249.3476307.
- [15] P. Fleith, "Controlled Anomalies Time Series (CATS) Dataset." Feb. 2023. doi: 10.5281/zenodo.7646897.
- [16] B. Ruszczak, K. Kotowski, D. Evans, and J. Nalepa, "The OPS-SAT benchmark for detecting anomalies in satellite telemetry," *Sci. Data*, vol. 12, no. 1, p. 710, Apr. 2025, doi: 10.1038/s41597-025-05035-3.
- [17] K. Kotowski, C. Haskamp, B. Ruszczak, J. Andrzejewski, and J. Nalepa, "Annotating Large Satellite Telemetry Dataset For ESA International AI Anomaly Detection Benchmark," in *Proceedings of the 2023 conference on Big Data from Space*, Vienna: Publications Office of the European Union, Nov. 2023, pp. 341–344. doi: 10.2760/46796.
- [18] S. Kim, K. Choi, H.-S. Choi, B. Lee, and S. Yoon, "Towards a Rigorous Evaluation of Time-Series Anomaly Detection," *Proc. AAAI Conf. Artif. Intell.*, vol. 36, no. 7, Art. no. 7, Jun. 2022, doi: 10.1609/aaai.v36i7.20680.
- [19] S. Sørbø and M. Ruocco, "Navigating the metric maze: a taxonomy of evaluation metrics for anomaly detection in time series," *Data Min. Knowl. Discov.*, Nov. 2023, doi: 10.1007/s10618-023-00988-8.
- [20] A. Lavin and S. Ahmad, "Evaluating Real-Time Anomaly Detection Algorithms The Numenta Anomaly Benchmark," in 2015 IEEE 14th International Conference on Machine Learning and Applications (ICMLA), Dec. 2015, pp. 38–44. doi: 10.1109/ICMLA.2015.141.
- [21] N. Singh and C. Olinsky, "Demystifying Numenta anomaly benchmark," in 2017 International Joint Conference on Neural Networks (IJCNN), May 2017, pp. 1570–1577. doi: 10.1109/IJCNN.2017.7966038.
- [22] H. Xu et al., "Unsupervised Anomaly Detection via Variational Auto-Encoder for Seasonal KPIs in Web Applications," in Proceedings of the 2018 World Wide Web Conference, in WWW '18. Republic and Canton of Geneva, CHE: International World Wide Web Conferences Steering Committee, Kwiecie 2018, pp. 187–196. doi: 10.1145/3178876.3185996.
- [23] W.-S. Hwang, J.-H. Yun, J. Kim, and B. G. Min, "Do you know existing accuracy metrics overrate time-series anomaly detections?," in *Proceedings of the 37th ACM/SIGAPP Symposium on Applied Computing*, Virtual Event: ACM, Apr. 2022, pp. 403–412. doi: 10.1145/3477314.3507024.
- [24] A. Huet, J. M. Navarro, and D. Rossi, "Local Evaluation of Time Series Anomaly Detection Algorithms," in *Proceedings of the 28th ACM SIGKDD Conference on Knowledge Discovery and Data Mining*, Washington DC USA: ACM, Aug. 2022, pp. 635–645. doi: 10.1145/3534678.3539339.
- [25] A. Abdulaal, Z. Liu, and T. Lancewicki, "Practical Approach to Asynchronous Multivariate Time Series Anomaly Detection and Localization," in *Proceedings of the 27th ACM SIGKDD Conference on Knowledge Discovery & Data Mining*, in KDD '21. New York, NY, USA: Association for Computing Machinery, Sierpie 2021, pp. 2485–2494. doi: 10.1145/3447548.3467174.

- [26] M. El Amine Sehili and Z. Zhang, "Multivariate Time Series Anomaly Detection: Fancy Algorithms and Flawed Evaluation Methodology," in *Performance Evaluation and Benchmarking*, R. Nambiar and M. Poess, Eds., Cham: Springer Nature Switzerland, 2024, pp. 1–17. doi: 10.1007/978-3-031-68031-1\_1.
- [27] A. Garg, W. Zhang, J. Samaran, R. Savitha, and C.-S. Foo, "An Evaluation of Anomaly Detection and Diagnosis in Multivariate Time Series," *IEEE Trans. Neural Netw. Learn. Syst.*, vol. 33, no. 6, pp. 2508–2517, Jun. 2022, doi: 10.1109/TNNLS.2021.3105827.
- [28] N. Tatbul, T. J. Lee, S. Zdonik, M. Alam, and J. Gottschlich, "Precision and Recall for Time Series," in *Advances in Neural Information Processing Systems*, Curran Associates, Inc., 2018. Accessed: Nov. 18, 2022. [Online]. Available: https://papers.nips.cc/paper/2018/hash/8f468c873a32bb0619eaeb2050ba45d1-Abstract.html
- [29] J. Paparrizos, P. Boniol, T. Palpanas, R. S. Tsay, A. Elmore, and M. J. Franklin, "Volume under the surface: a new accuracy evaluation measure for time-series anomaly detection," *Proc. VLDB Endow.*, vol. 15, no. 11, pp. 2774–2787, Jul. 2022, doi: 10.14778/3551793.3551830.
- [30] T. S. Buda, H. Assem, and L. Xu, "ADE: An ensemble approach for early Anomaly Detection," in 2017 IFIP/IEEE Symposium on Integrated Network and Service Management (IM), 2017, pp. 442–448.
- [31] J. Nalepa, M. Myller, J. Andrzejewski, P. Benecki, S. Piechaczek, and D. Kostrzewa, "Evaluating algorithms for anomaly detection in satellite telemetry data," *Acta Astronaut.*, Jun. 2022, doi: 10.1016/j.actaastro.2022.06.026.
- [32] K. Järvelin and J. Kekäläinen, "Cumulated gain-based evaluation of IR techniques," ACM Trans. Inf. Syst., vol. 20, no. 4, pp. 422–446, Październik 2002, doi: 10.1145/582415.582418.
- [33] H. Zhao *et al.*, "Multivariate Time-Series Anomaly Detection via Graph Attention Network," in 2020 IEEE International Conference on Data Mining (ICDM), Nov. 2020, pp. 841–850. doi: 10.1109/ICDM50108.2020.00093.
- [34] S. Tuli, G. Casale, and N. R. Jennings, "TranAD: deep transformer networks for anomaly detection in multivariate time series data," Proc. VLDB Endow., vol. 15, no. 6, pp. 1201–1214, Luty 2022, doi: 10.14778/3514061.3514067.
- [35] P. Benecki, S. Piechaczek, D. Kostrzewa, and J. Nalepa, "Detecting Anomalies in Spacecraft Telemetry Using Evolutionary Thresholding and LSTMs," in *Proceedings of the Genetic and Evolutionary Computation Conference Companion*, New York, NY, USA: ACM, 2021, pp. 143–144.
- [36] E. W. Grafarend, *Linear and nonlinear models: fixed effects, random effects, and mixed models*. Berlin; New York: Walter de Gruyter, 2006. Accessed: Nov. 22, 2022. [Online]. Available: http://archive.org/details/linearnonlinearm00wgra
- [37] J. Xu, H. Wu, J. Wang, and M. Long, "Anomaly Transformer: Time Series Anomaly Detection with Association Discrepancy," Oct. 2021, doi: 10.48550/arXiv.2110.02642.
- [38] Y. Zhao, Z. Nasrullah, and Z. Li, "PyOD: A Python Toolbox for Scalable Outlier Detection," *J. Mach. Learn. Res.*, vol. 20, no. 96, pp. 1–7, 2019.
- [39] M.-L. Shyu, S.-C. Chen, K. Sarinnapakorn, and L. Chang, "A novel anomaly detection scheme based on principal component classifier," Miami Univ Coral Gables Fl Dept of Electrical and Computer Engineering, 2003.
- [40] M. Goldstein and A. Dengel, "Histogram-based Outlier Score (HBOS): A fast Unsupervised Anomaly Detection Algorithm," in 35th German Conference on Artificial Intelligence, Saarbrucken, 2012.
- [41] F. T. Liu, K. M. Ting, and Z.-H. Zhou, "Isolation Forest," in *Proceedings of the 2008 Eighth IEEE International Conference on Data Mining*, in ICDM '08. USA: IEEE Computer Society, Grudzie 2008, pp. 413–422. doi: 10.1109/ICDM.2008.17.
- [42] S. Ramaswamy, R. Rastogi, and K. Shim, "Efficient algorithms for mining outliers from large data sets," *ACM SIGMOD Rec.*, vol. 29, no. 2, pp. 427–438, Maj 2000, doi: 10.1145/335191.335437.
- [43] Y. Lu, R. Wu, A. Mueen, M. A. Zuluaga, and E. Keogh, "DAMP: accurate time series anomaly detection on trillions of datapoints and ultra-fast arriving data streams," *Data Min. Knowl. Discov.*, vol. 37, no. 2, pp. 627–669, Mar. 2023, doi: 10.1007/s10618-022-00911-7.
- [44] Y. Lu, M. Imamura, T. V. A. Srinivas, E. Keogh, and T. Nakamura, "Matrix Profile XXX: MADRID: A Hyper-Anytime and Parameter-Free Algorithm to Find Time Series Anomalies of all Lengths (In Press)," in *IEEE International Conference on Data Mining*, Shanghai, Dec. 2023.
- [45] C.-C. M. Yeh, N. Kavantzas, and E. Keogh, "Matrix Profile VI: Meaningful Multidimensional Motif Discovery," in 2017 IEEE International Conference on Data Mining (ICDM), New Orleans, LA: IEEE, Nov. 2017, pp. 565–574. doi: 10.1109/ICDM.2017.66.
- [46] M. M. Breunig, H.-P. Kriegel, R. T. Ng, and J. Sander, "LOF: identifying density-based local outliers," in *Proceedings of the 2000 ACM SIGMOD international conference on Management of data*, in SIGMOD '00. New York, NY, USA: Association for Computing Machinery, Maj 2000, pp. 93–104. doi: 10.1145/342009.335388.
- [47] T. Yairi, Y. Kato, and K. Hori, "Fault detection by mining association rules from house-keeping data," presented at the Proceedings of the 6th International Symposium on Artificial Intelligence, Robotics and Automation in Space, Quebec, 2001, p. 21. [Online]. Available: https://robotics.estec.esa.int/i-SAIRAS/isairas2001/papers/Paper\_AS012.pdf
- [48] N. Heim and J. E. Avery, "Adaptive Anomaly Detection in Chaotic Time Series with a Spatially Aware Echo State Network," Sep. 02, 2019, arXiv: arXiv:1909.01709. doi: 10.48550/arXiv.1909.01709.
- [49] R. Paffenroth, K. Kay, and L. Servi, "Robust PCA for Anomaly Detection in Cyber Networks," Jan. 04, 2018, arXiv: arXiv:1801.01571. doi: 10.48550/arXiv.1801.01571.
- [50] Z. Li, Y. Zhao, N. Botta, C. Ionescu, and X. Hu, "COPOD: Copula-Based Outlier Detection," in 2020 IEEE International Conference on Data Mining (ICDM), Nov. 2020, pp. 1118–1123. doi: 10.1109/ICDM50108.2020.00135.
- [51] M. Sakurada and T. Yairi, "Anomaly Detection Using Autoencoders with Nonlinear Dimensionality Reduction," in *Proceedings of the MLSDA 2014 2nd Workshop on Machine Learning for Sensory Data Analysis*, in MLSDA'14. New York, NY, USA: Association for Computing Machinery, Grudzie 2014, pp. 4–11. doi: 10.1145/2689746.2689747.
- [52] H. J. Song Zhuqing; Men, Aidong; Yang, Bo, "A Hybrid Semi-Supervised Anomaly Detection Model for High-Dimensional Data," Comput. Intell. Neurosci., vol. 2017, no. NA, pp. 8501683–8501683, 2017, doi: 10.1155/2017/8501683.
- [53] P. Malhotra, L. Vig, G. Shroff, and P. Agarwal, "Long short term memory networks for anomaly detection in time series," in *European Symposium on Artificial Neural Networks, Computational Intelligence and Machine Learning*, Bruges, 2015, pp. 89–94.
- [54] P. Wenig, S. Schmidl, and T. Papenbrock, "TimeEval: a benchmarking toolkit for time series anomaly detection algorithms," *Proc. VLDB Endow.*, vol. 15, no. 12, pp. 3678–3681, Sep. 2022, doi: 10.14778/3554821.3554873.

[55] J. Nalepa *et al.*, "Toward On-Board Detection Of Anomalous Events From Ops-Sat Telemetry Using Deep Learning," in 8th International Workshop On On-Board Payload Data Compression, Athens: Zenodo, 2022. doi: 10.5281/zenodo.724499.